Institute of Physics of Materials,
Czech Academy of Sciences

Žižkova 22, Brno, Czech Republic

SIRAMM, January 2021

Fatigue Properties of Metallic Materials Produced by Additive Manufacturing

Ludvík Kunz

Institute of Physics of Materials, Czech Academy of Sciences, Brno, Czech Republic,

1st Winter School on

Trends on Additive Manufacturing for Engineering Applications

Institute of Physics of Materials, Czech Academy of Sciences, Brno, Czech Republic

University of Parma, Parma, Italy
prof. Gianni Nicoletto,
Department of Engineering and Architecture

Additive manufacturing

- Quickly developing production technology based on **joining of materials layer upon layer** to produce objects from 3D models

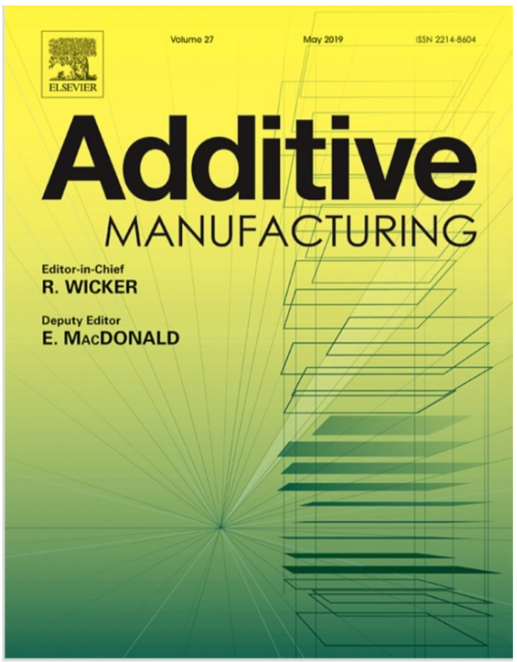

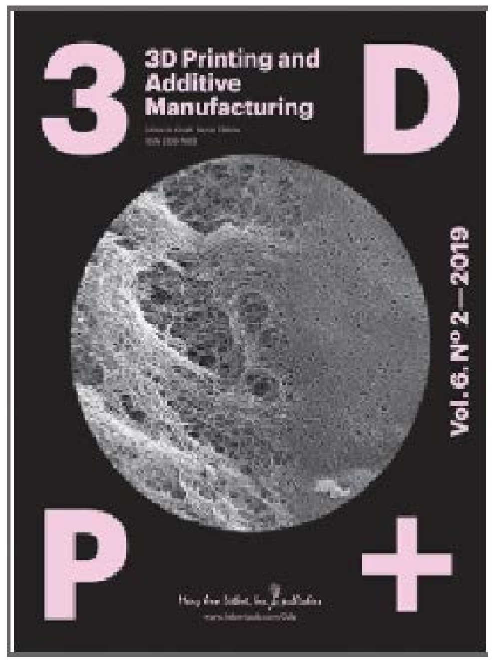

A lot of papers in scientific journals, many conferences and many specialized books

Additive manufacturing

Web of Science

Yesterday:

Topic „Additive manufacturing“	in 2020	6100 results
	in 2021	295 results
„Metal laser sintering“	in 2020	211 results

SCOPUS

Topic „Additive manufacturing“	in 2020	29 807 results
	all years	135 901 results

Next industrial revolution?

Additive manufacturing

History

- additive manufacturing technology patented in 1971

- concept of Selective Laser Sintering systems, which concerned moulding processes in the creation of 3D models in layers patented 1979

- since the end of the 90's: sharp acceleration
  - computer technology
  - friendly designed software
  - interfaces to AM process
  - laser technology
  - electron beam technology

Additive manufacturing

- Materials – **polymers, metals, ceramics**
- Obvious **advantages:**

  listed this morning by prof. Torgersen

  - manufacturing of parts directly from a CAD file
  - rapid prototyping
  - building of components with complex shape with internal features
  - minimum material waste
  - suitable for fabrication of small series of products (not necessary to use expensive tools and implements)

Additive manufacturing of metals

- **Drawbacks and shortcomings:**
  - very complex technology
  - many processing parameters influencing the quality of products
  - expensive (printing metals)
  - rough surface finish
  - lots of post-processing required
  - not enough knowledge and experience, further manufacturing skills needed

The fatigue behaviour, failure criteria and failure prediction of DMLS materials has to be thoroughly assessed

Polymers

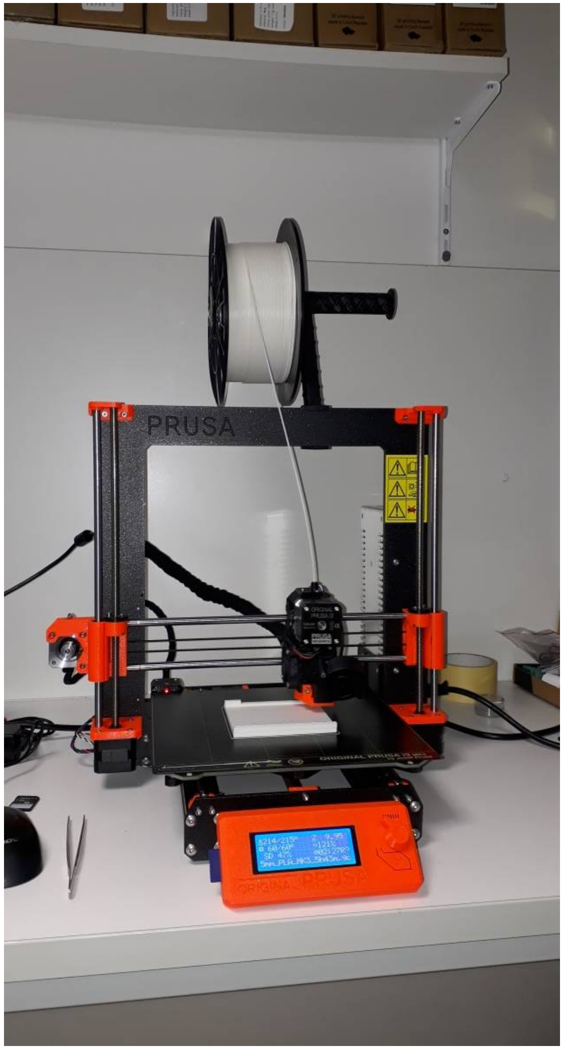

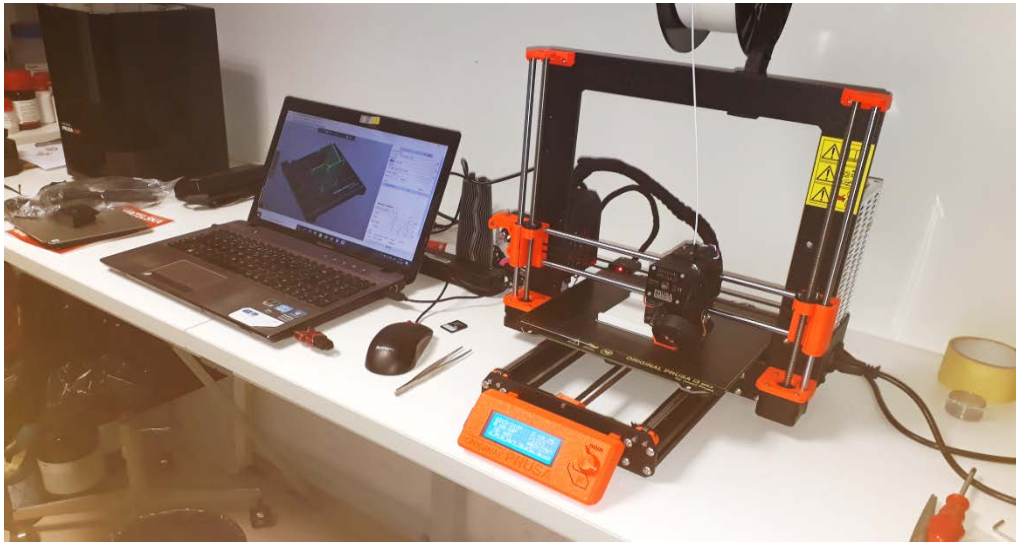

Prusa i3 MK3S+ 3D printer
mentioned this morning by prof. Marsavina

Czech company
production: 9000 printers/month
cost: 300 - 700 EUR

Polymers

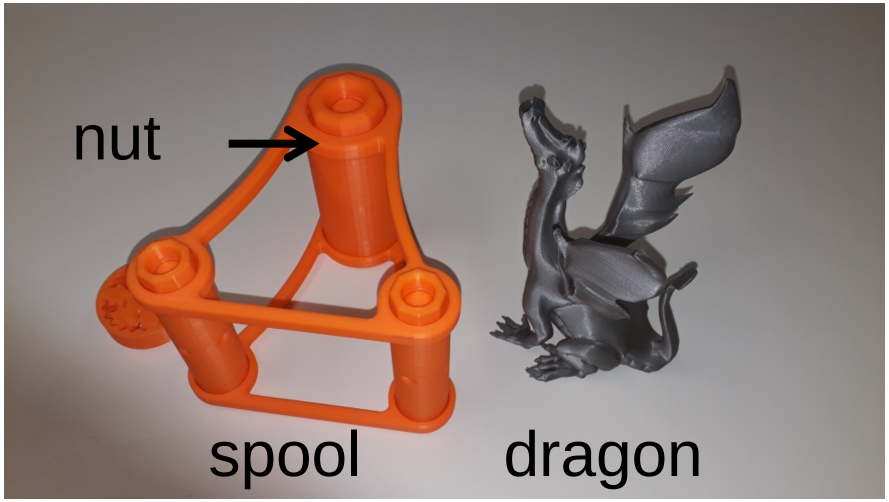

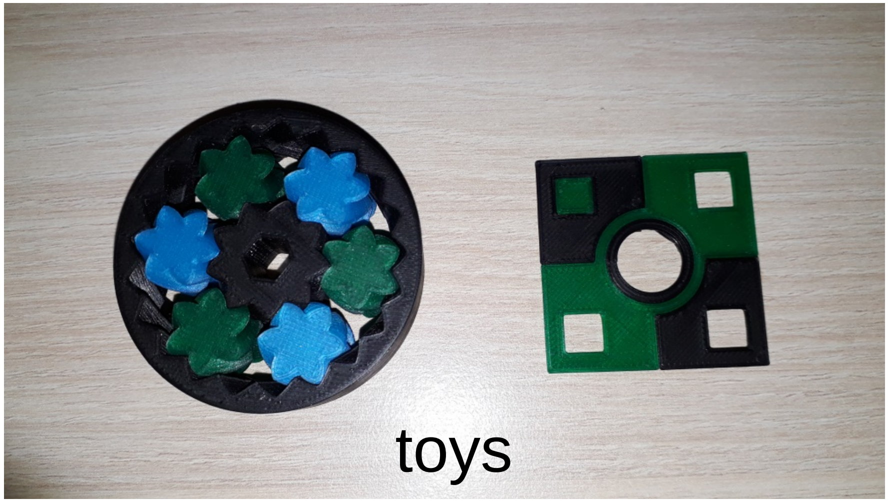

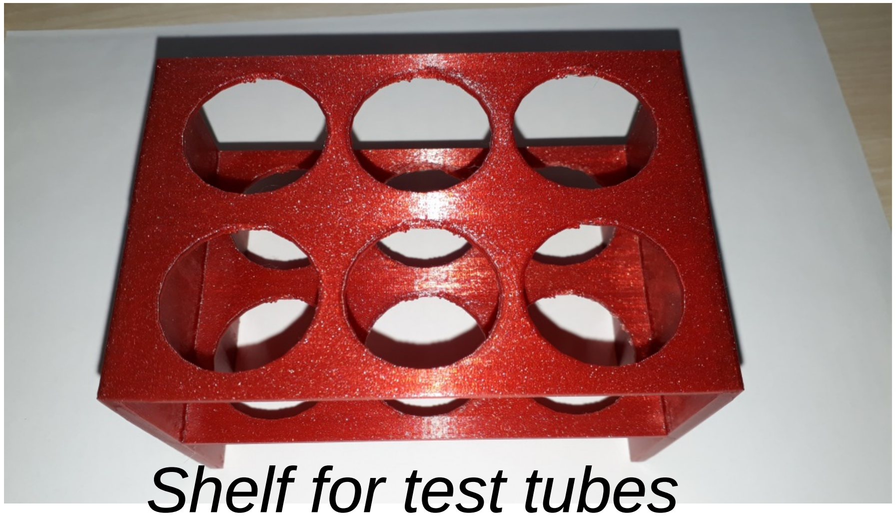

Examples of printed objects from plastics

Metals
Ti6Al4V components

lightweight turbine cover door hinge for Airbus

http://www.materialstoday.com/additive-manufacturing/news/eos-method-for-specifying-am-parameters/

spinal implants

http://www.prototypetoday.com/news/press-releases/eos/Page-2

Additive manufacturing of metals

Powder bed technologies

- Laser Beam Melting (LMB)
  - **Direct Metal Laser Sintering (DMLS)**
- Electron Beam Melting (EBM)

Powder deposition technologies

- Laser Engineered Net Shaping (LENS)
- Direct Metal Deposition (DMD)
- Laser Cladding

Additive manufacturing

Direct metal laser sintering (DMLS): one of the most often used powder bed fusion techniques

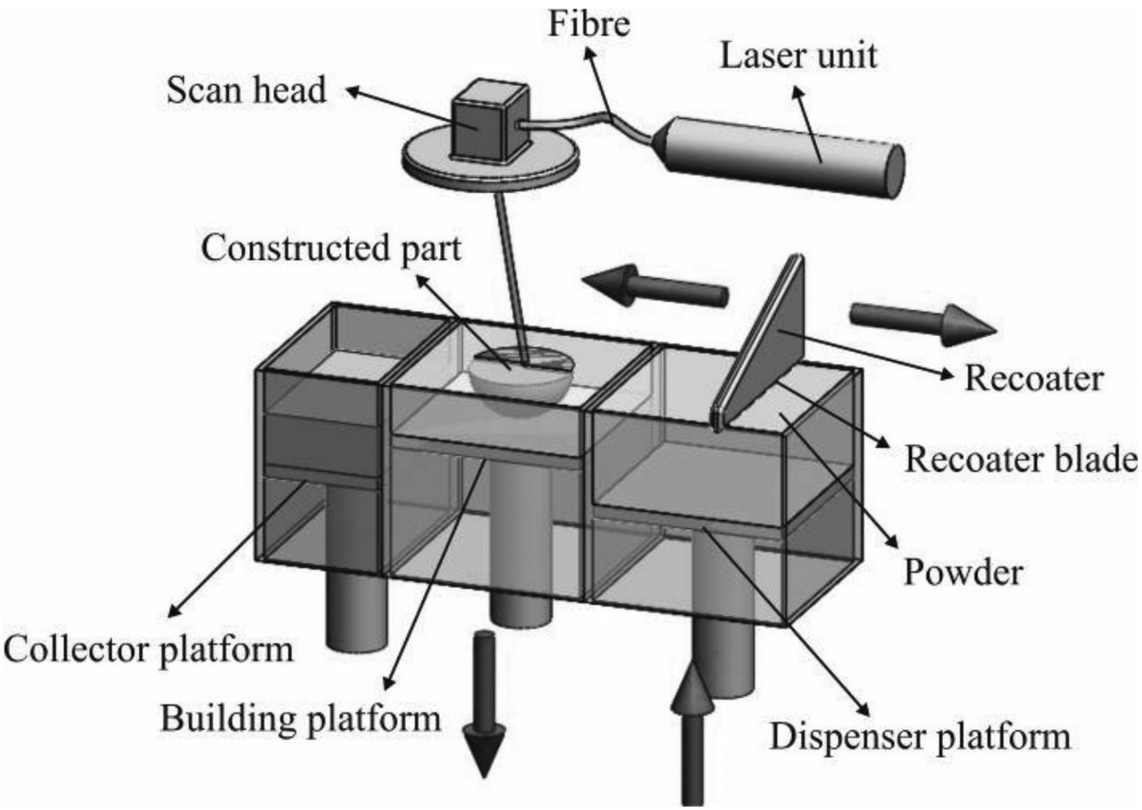

Identical principle was presented in the preceding talk by prof. Spagnoli for polymeric materials

Schematic diagram of the DMLS system. Longhitano et al.: 2015; 18(4): 838-842 /

Additive manufacturing

RENISHAW A250 **EOSINT M 270** **SLM 280 HL**

Cost: hundreds of thousands to millions of EUR

Direct metal laser sintering

Properties of DMLS materials are strongly dependent on processing parameters

- input powder
- laser scanning strategy
- energy density
- scan speed
- laser power
- layer thickness
- build orientation
- component size and shape
- location on building plate
- build platform heating
- final heat treatment

attention to material properties and structure must be paid !

DMLS manufactured materials

Ti alloy Ti6Al4V:

- aerospace
- medicine
- chemical industry

low weight,
high strength,
biocompatibility
corrosion resistance

IN 718 superalloy:

- high temperature industrial applications

excellent high temperature and cryogenic properties

Direct metal laser sintering

- process is prone to **porosity** and **defects** arising from lack of fusion and thermal stresses
- **uneven defect distribution** in component
- **directionality of structure** (anisotropy) due to layer wise building
- **high residual stresses**
- **surface quality** dependent on building direction

Defects in Ti6Al4V

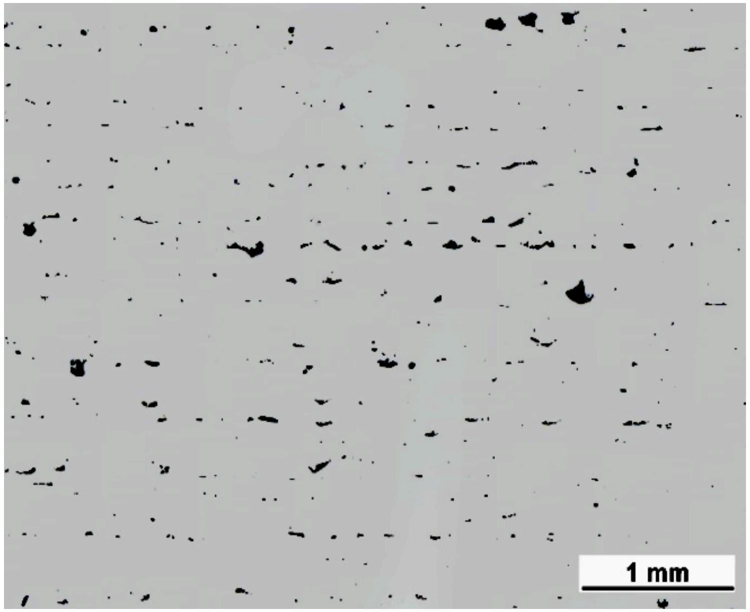

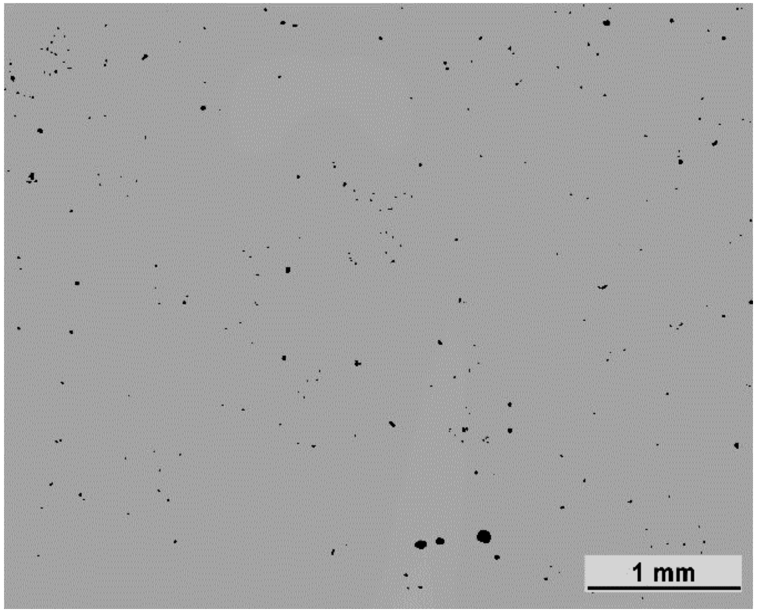

non-optimally set parameters

RENISHAW AM 250

linear defects distribution

average porosity 3.87 %

optimally set parameters

EOSINT M270

random defects distribution

average porosity 0.24 %

Defects can be substantially reduced by optimization of processing parameters

Defects in **Ti6Al4V**

Process-driven defects: fusion voids, gas pores, partially-/un-melted powder particles, cracks

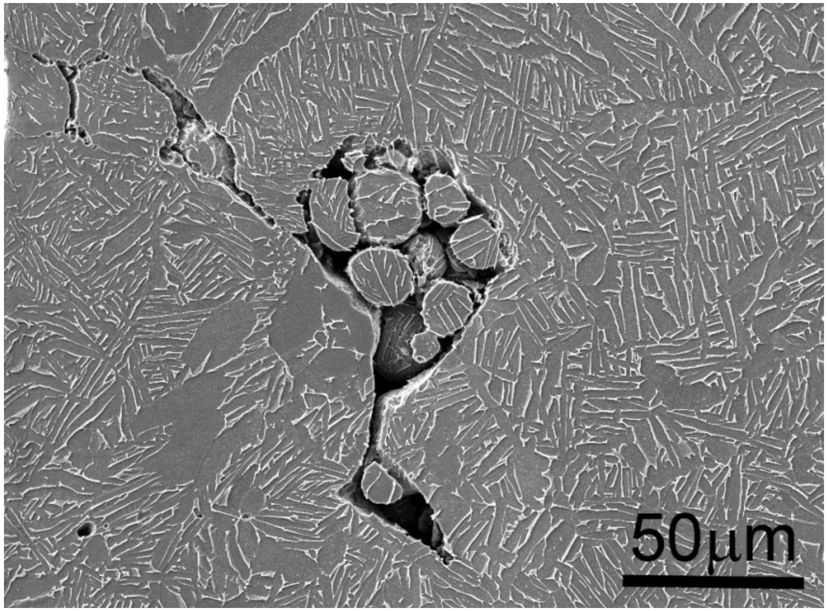

Unmelted particles

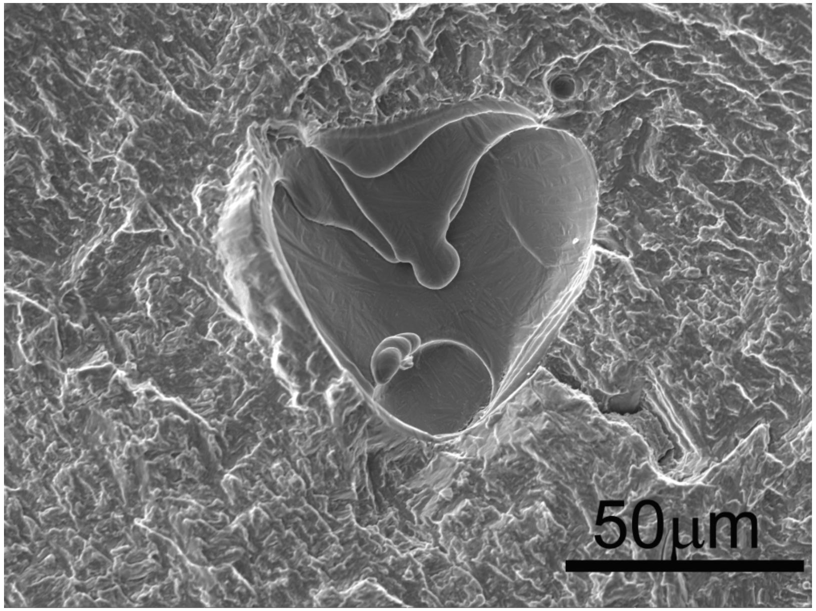

Void on fatigue fracture surface

Post processing treatment Hot isostatic pressing is often applied

Density 99.8 % can be achieved when HIP is applied

Defects in **IN 718**

Process-driven defects: fusion voids, gas pores, partially-/un-melted powder particles, cracks

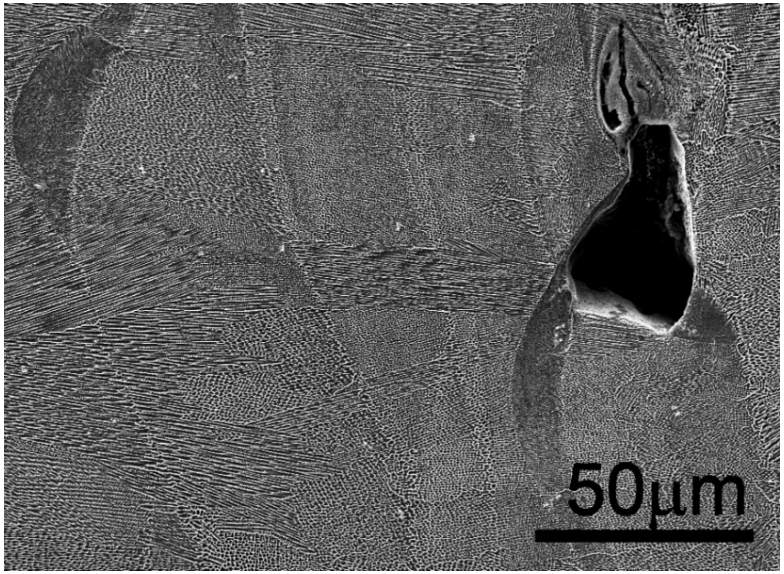

Characteristic fusion void

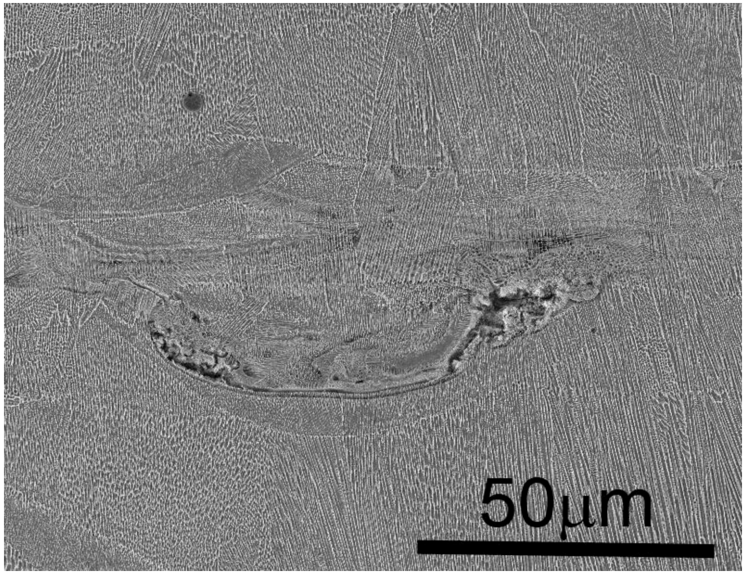

Defect along melt pool line

Small defects cannot be removed completely

Direct metal laser sintering

- process is prone to porosity and defects arising from lack of fusion and thermal stresses
- uneven defect distribution in component
- **directionality of structure** (anisotropy) due to layer wise building
- high residual stresses
- surface quality dependent on building direction

Directionality of structure of **Ti6Al4V**

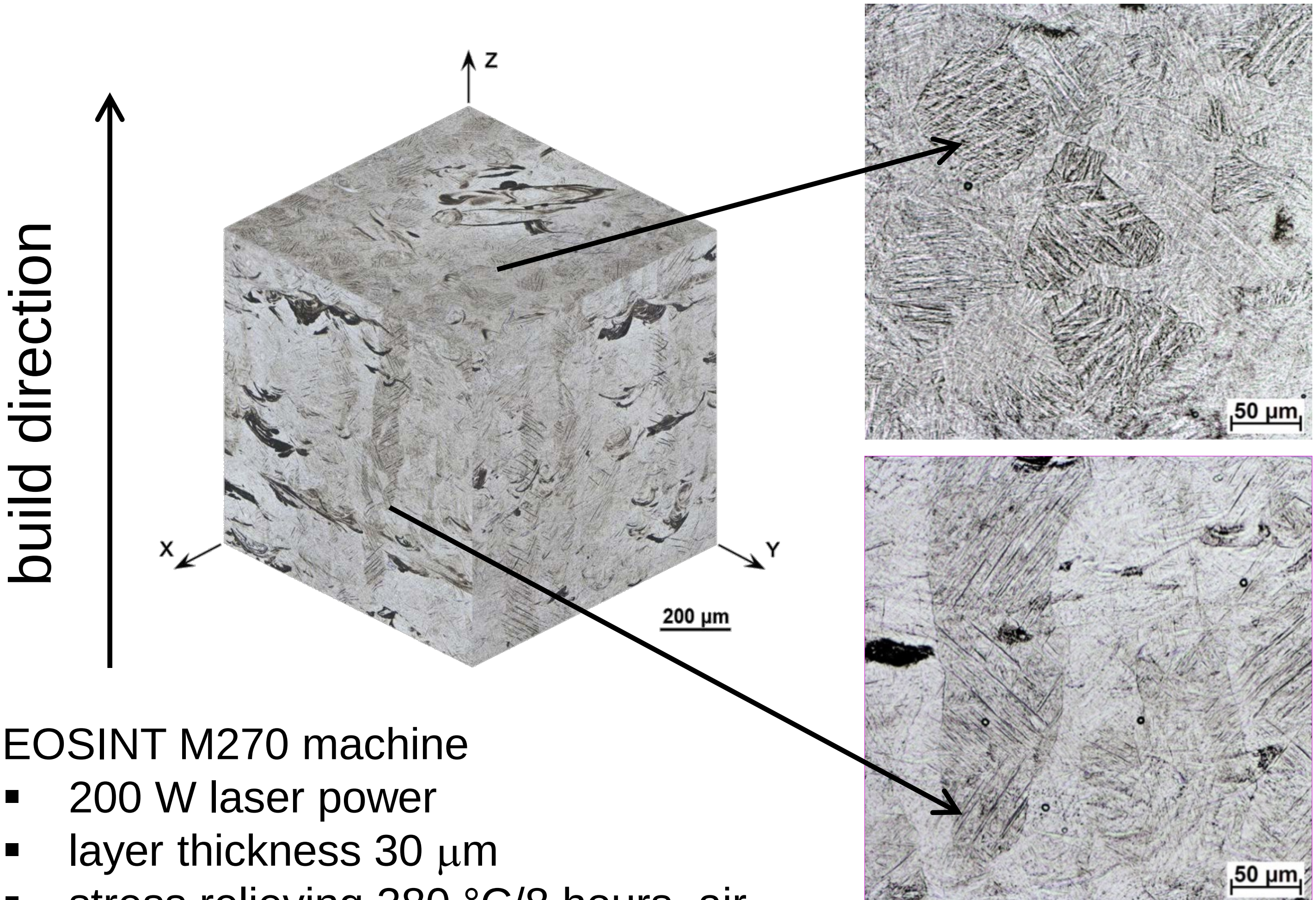

EOSINT M270 machine

- 200 W laser power
- layer thickness 30 μm
- stress relieving 380 °C/8 hours, air

Columnar grains in building direction, epitaxial growth

Directionality of structure of **IN 718**

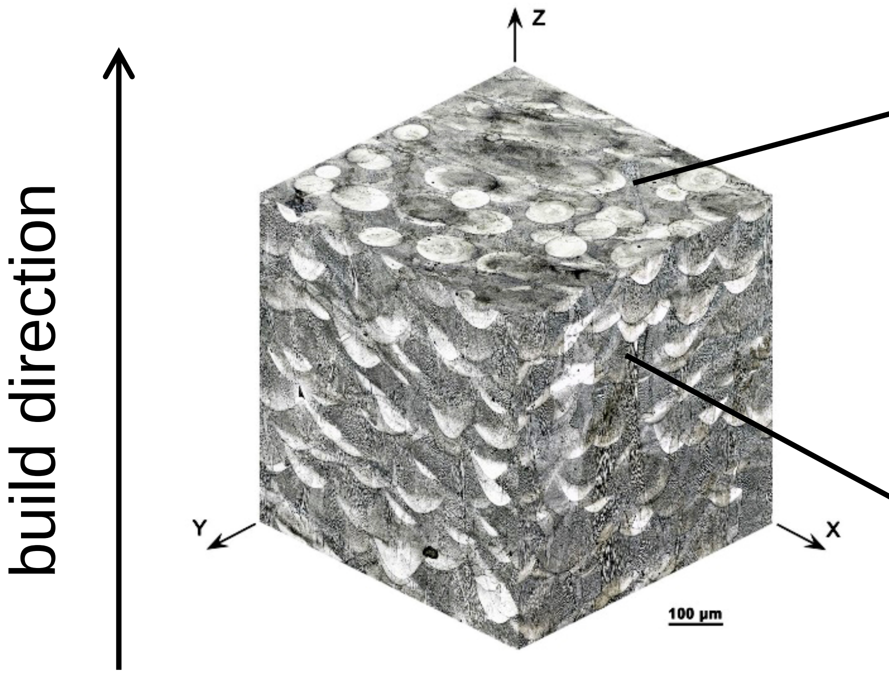

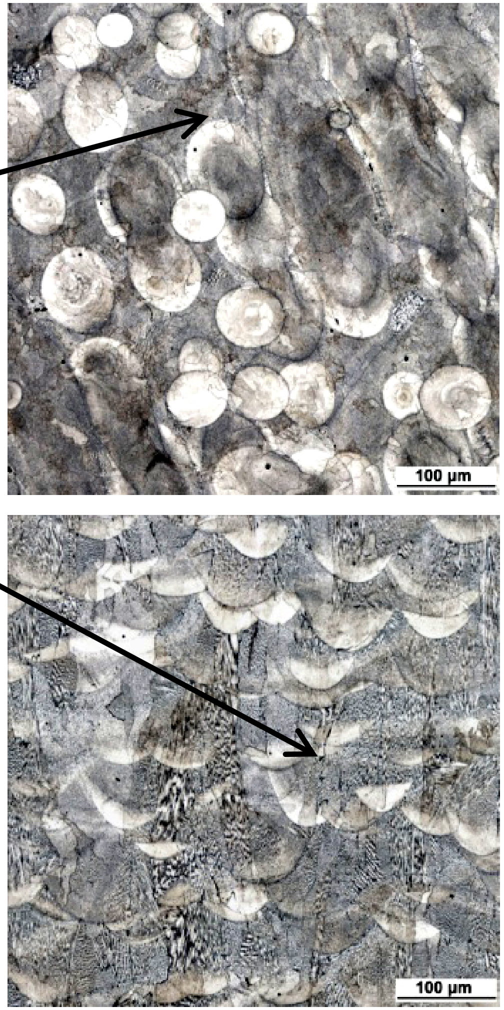

RENISHAW AM 250 machine

- 200 W laser power
- layer thickness 50 μm
- as-built state

The structure exhibits directionality

Direct metal laser sintering

- process is prone to porosity and defects arising from lack of fusion and thermal stresses
- uneven defect distribution in component
- directionality of structure (anisotropy) due to layer wise building
- **high residual stresses**
- surface quality dependent on building direction

Residual stresses

develops due to rapid heating and cooling

can result in deformation and failure

- within the additive process
- in post processing steps

influence on dimensional accuracy, distortions

residual stresses

- type I – macroscale (most important)
- type II – microscale – between individual grains
- type III – sub microscale – inside grains

Residual stresses

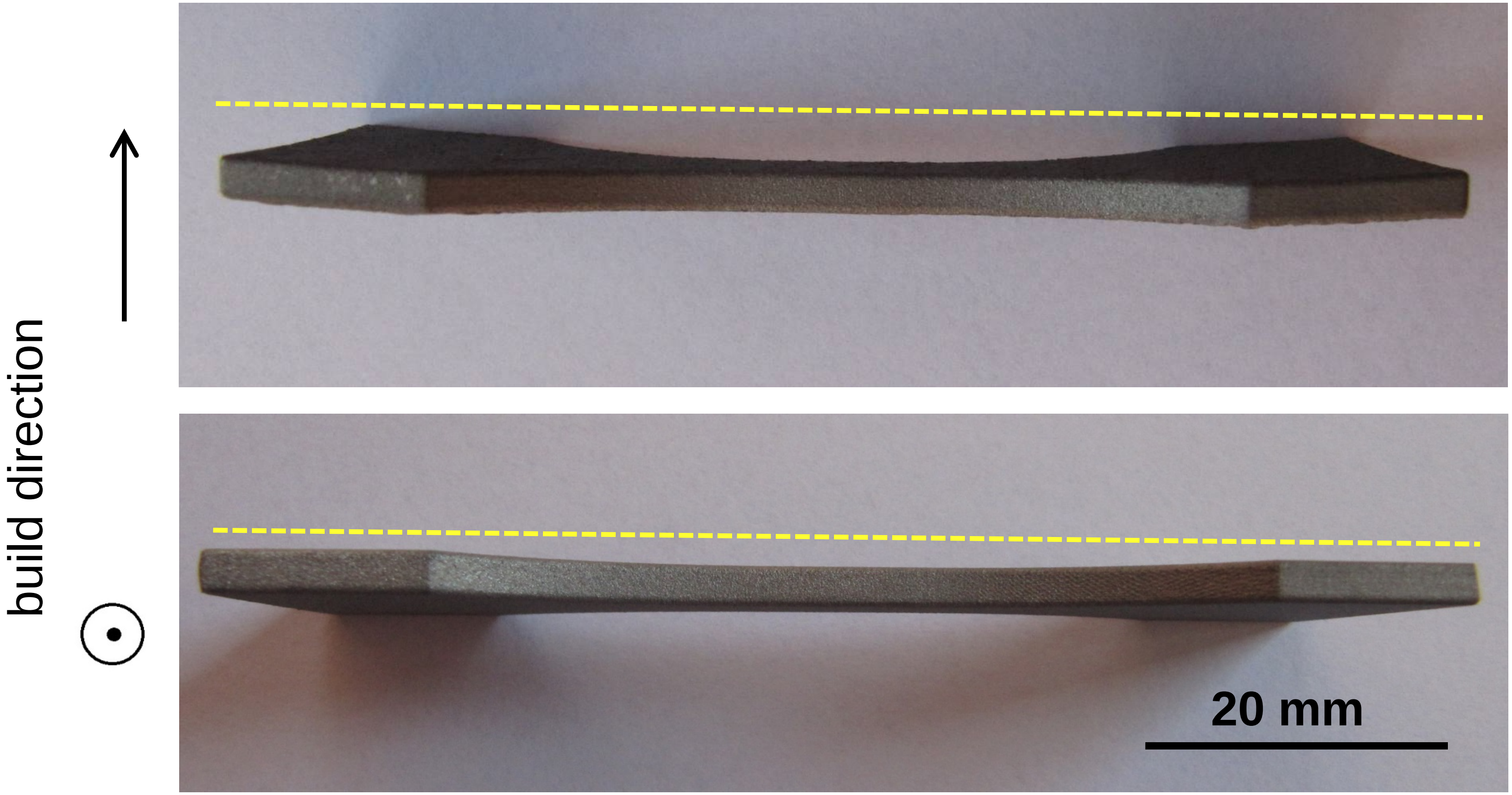

Ti6Al4V specimens removed from platform without stress relieving by cutting off the supports

Stress relieving is a necessary post processing step

Direct metal laser sintering

- process is prone to porosity arising from lack of fusion and thermal stresses
- uneven pore distribution in component
- directionality of structure (anisotropy) due to layer wise building
- high residual stresses
- **surface quality** dependent on building direction

Surface quality of **Ti6Al4V**

- strongly depends on building orientation
- depends on scanning strategy

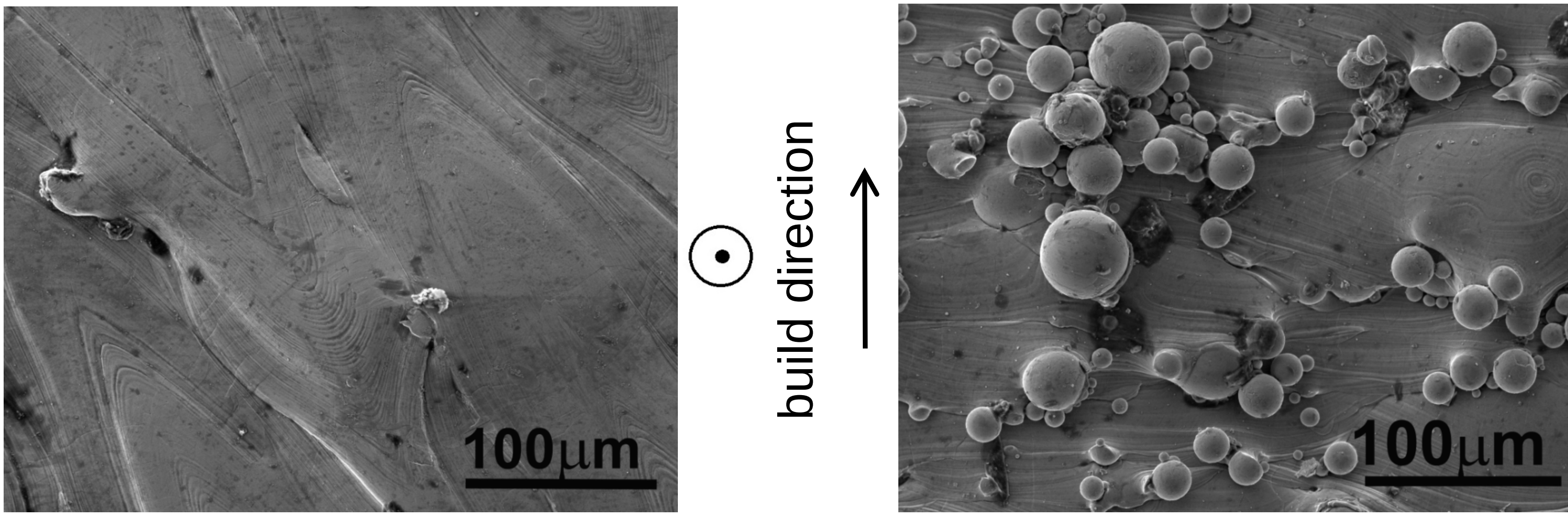

EOSINT M290 machine

- 400 W laser power
- layer thickness 60 μm
- scanning strategy BEAM-IT

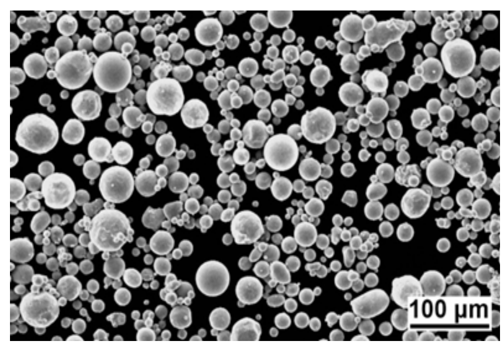

Ti6Al4V powder
average particle size
30 - 34 μm

Surface quality of **Ti6Al4V**

build direction

specimen for fatigue test

as-built surface

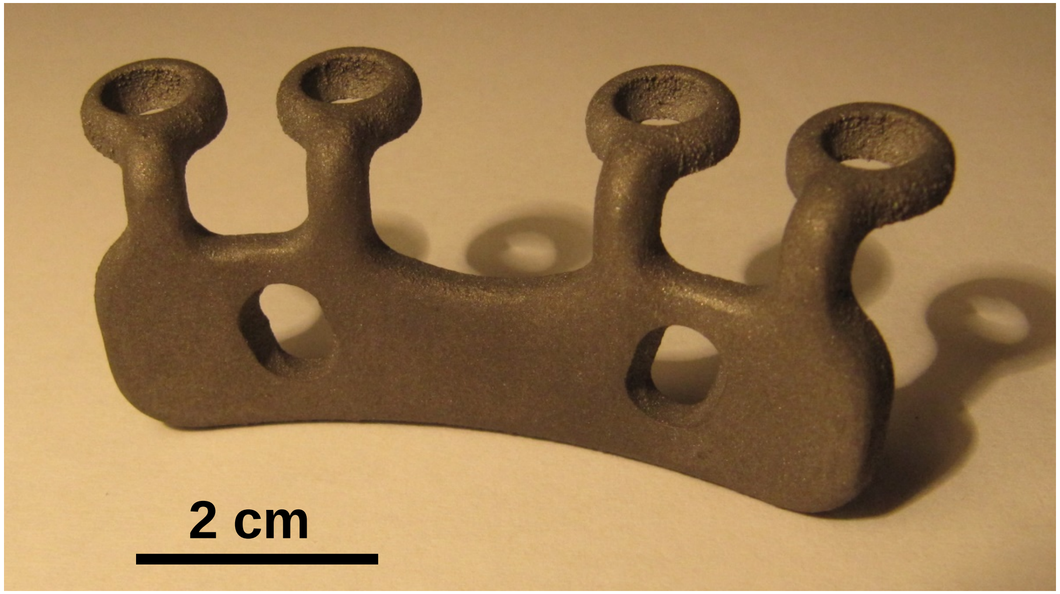

symphysis clasp

surface finished by shot peening

Surface quality of IN 718

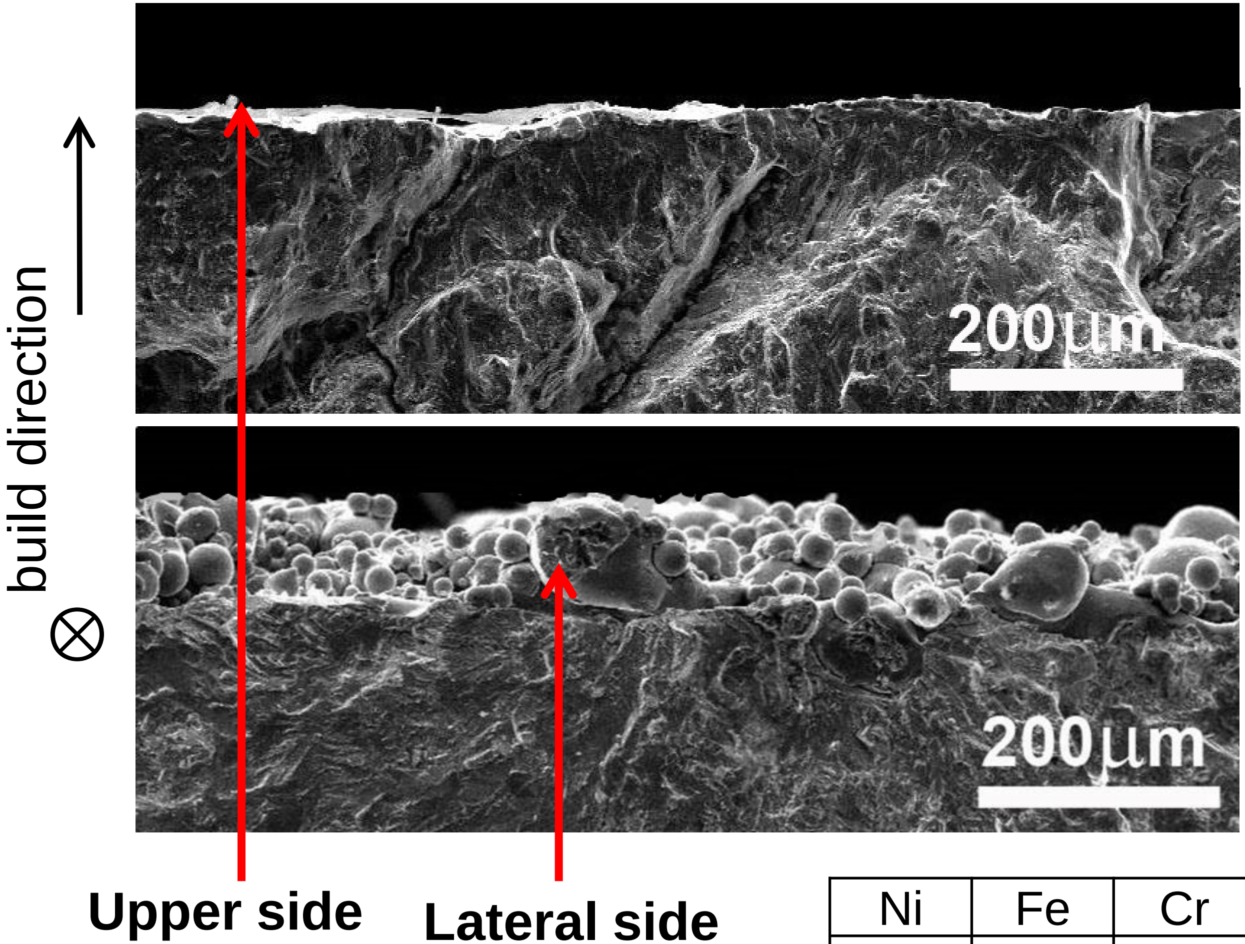

RENISHAW 250

- 200 W laser power
- layer thickness 30 µm
- scanning strategy BEAM-IT
- Powder particle size 24-53 µm

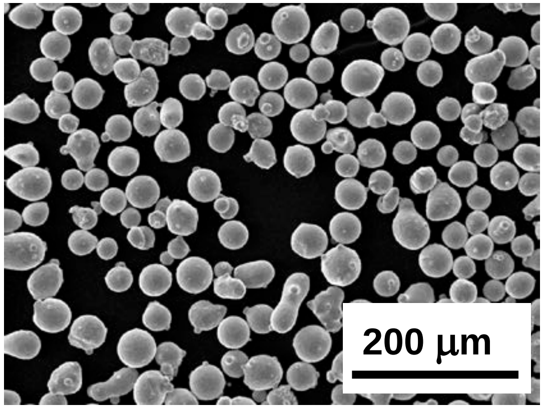

Ni	Fe	Cr	Nb	Mo	Ti	Al
52.5	18.4	19.9	5.1	3.22	0.92	0.71

As-built surface roughness strongly depends on the orientation

Fatigue properties of DMLS materials

- defects
- inhomogeneity and directionality of microstructure
- residual stresses
- surface roughness

→

- **fatigue strength and fatigue limit**
- **long fatigue crack growth and threshold values**

Fatigue strength and fatigue limit
Ti6Al4V

S-N curves

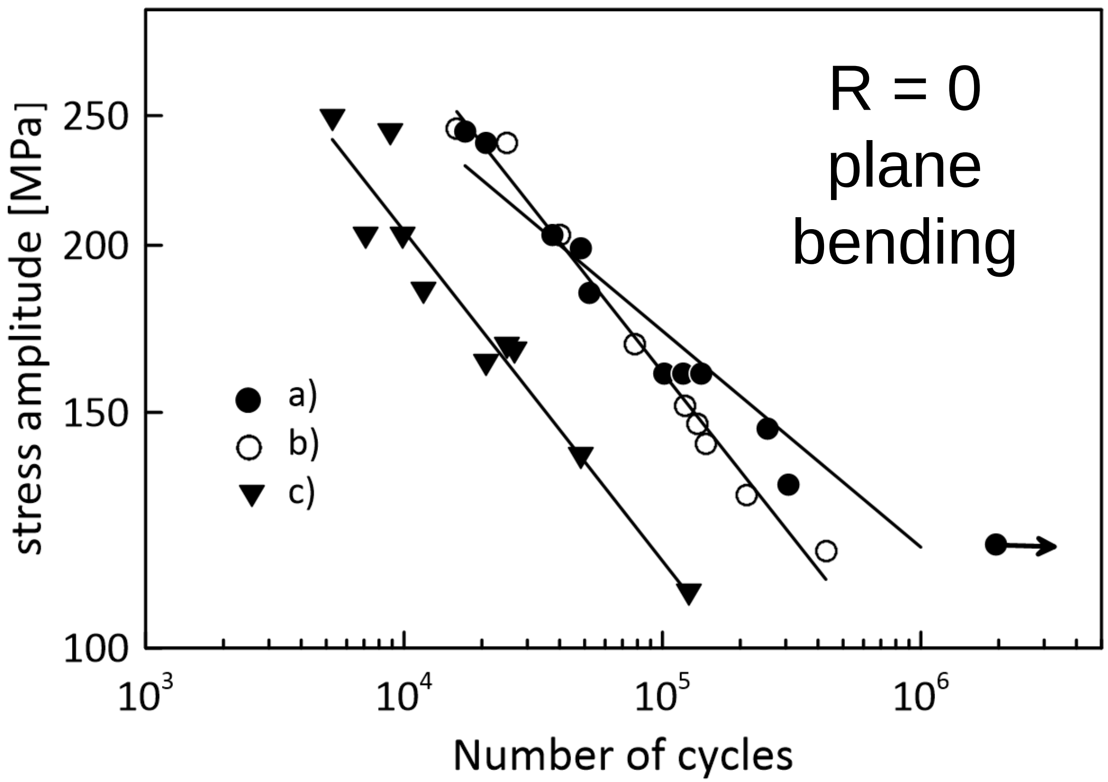

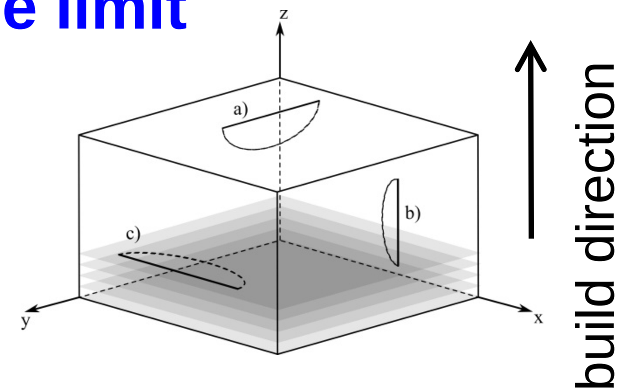

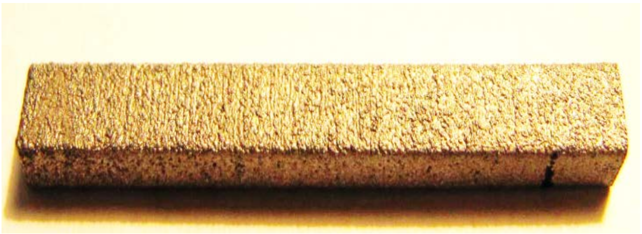

Specimen for plane bending

- **Fatigue performance depends on the build orientation**
- **Lowest fatigue strength exhibits orientation *c***

EOSINT M270 machine

- 200 W laser power
- layer thickness 30 μm
- multi-directional scan strategy (rotation of scan direction)
- stress relieving 380 °C/8 hours, air

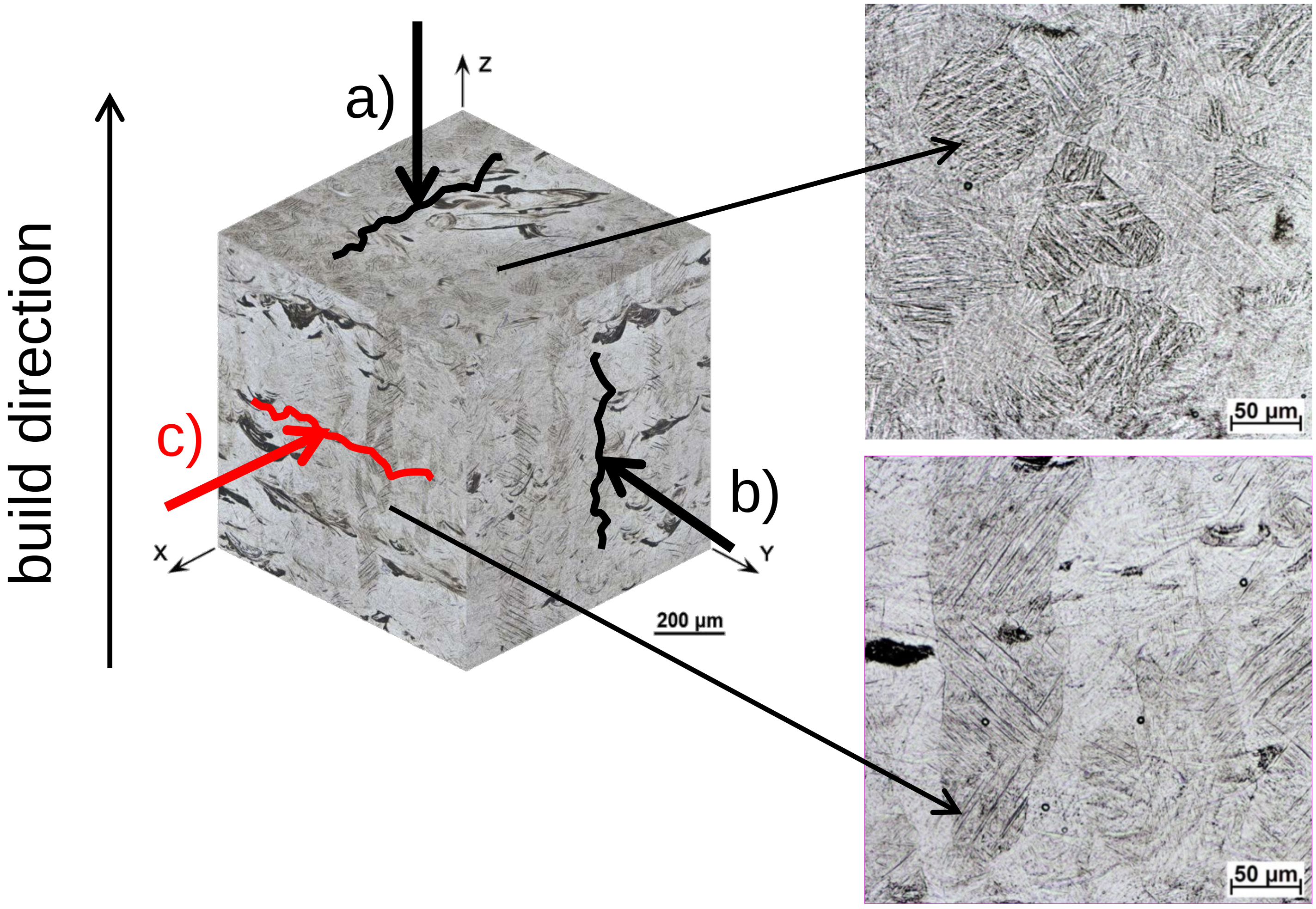
build direction
a)
b)
c)
z
x
Y
200 µm
50 µm
50 µm

Fatigue strength and fatigue limit IN 718

S-N curves

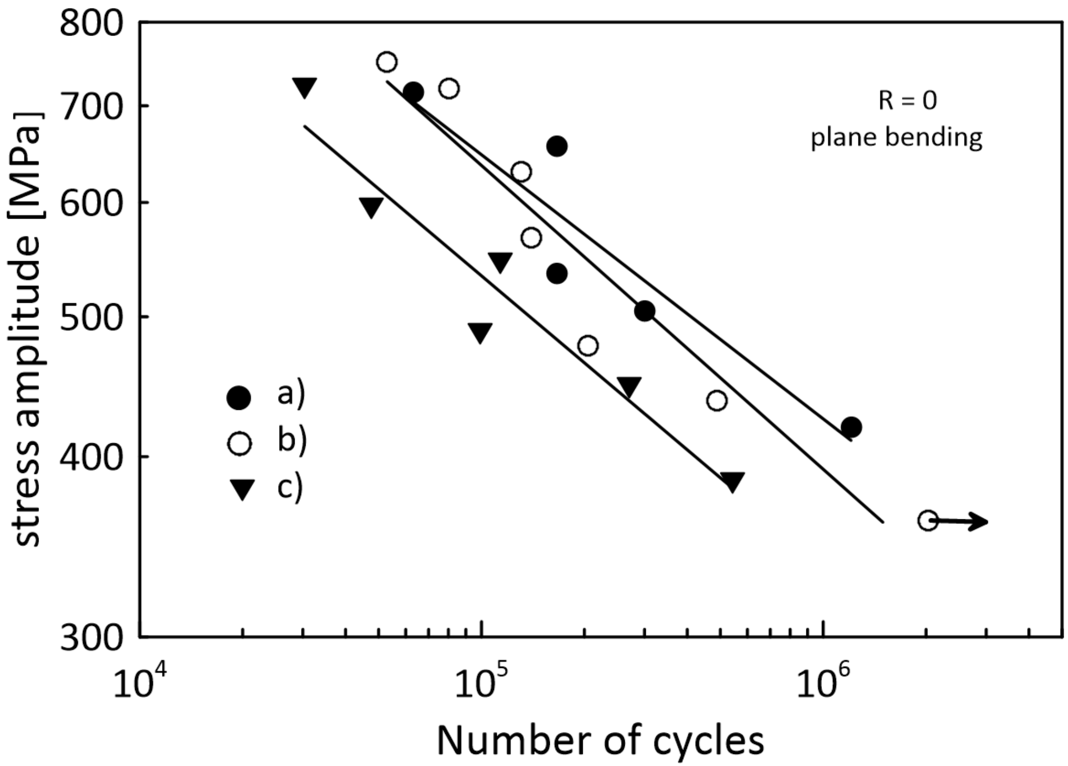

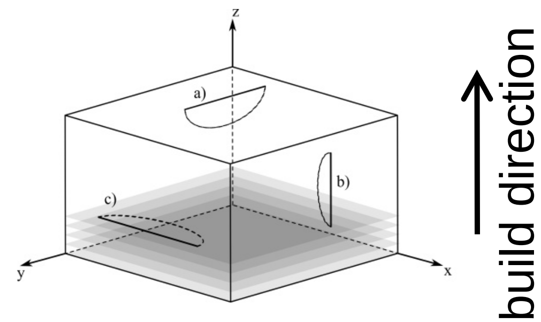

RENISHAW 250

- 200 W laser power
- layer thickness 30 µm
- scanning strategy BEAM-IT
- heat treatment: 970 °C/1h, cooling in Ar, age hardening 710 °C/8 h, 610 °C/8 h

- **Fatigue performance depends on the build orientation**
- **Lowest fatigue strength exhibits orientation *c***

IN 718

Fatigue fracture surfaces

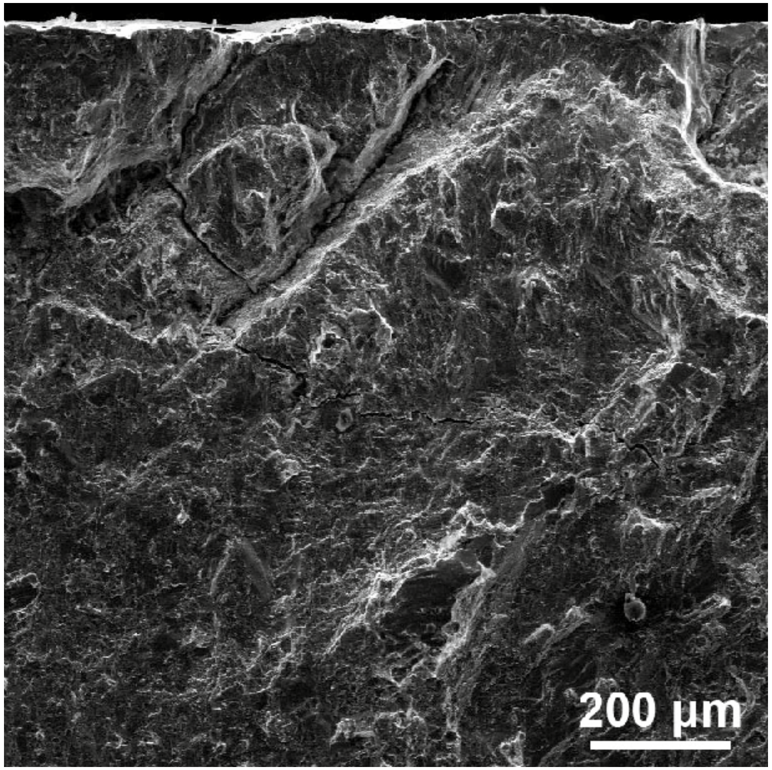

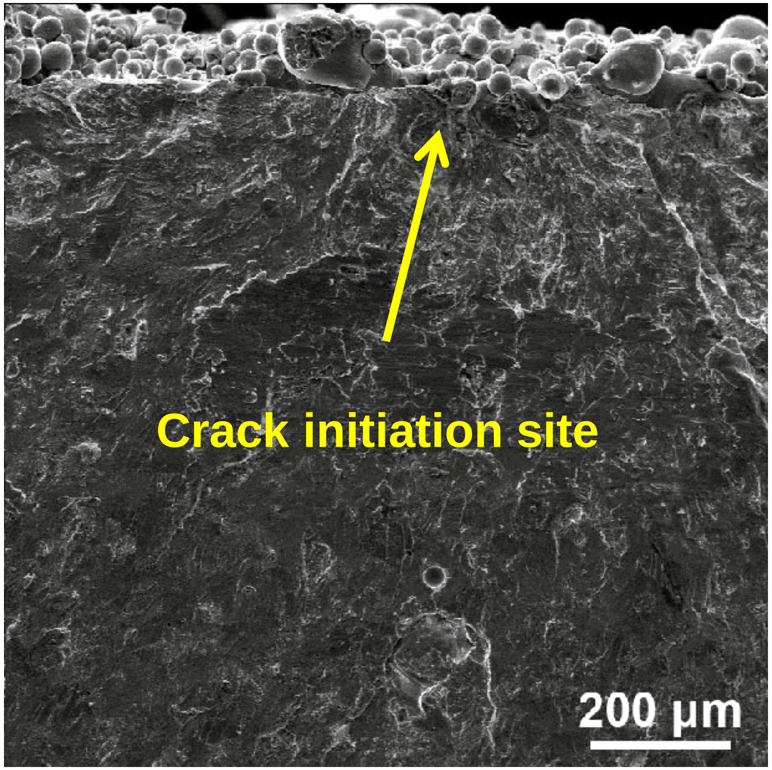

orientation a) higher fatigue life

orientation c) lower fatgiue life

Surface roughness determines the fatigue life (when internal defects are minimalized by optimization of processing parameters)

Long fatigue crack growth and threshold values

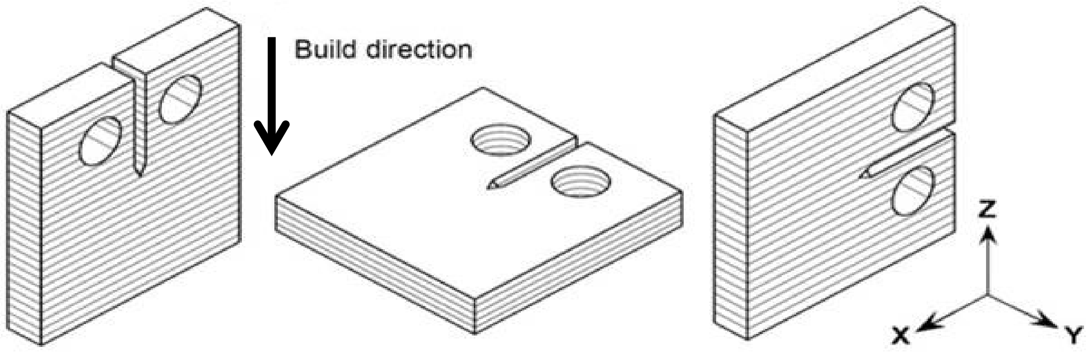

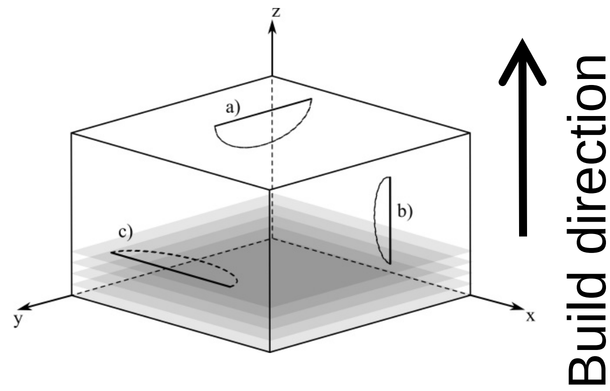

a) ***b)*** ***c)***

orientation

a): crack growth perpendicular to layers and in build direction

b): crack growth perpendicular to layers and in plain parallel to build direction

c): crack growth along the layers (perpendicular to build direction)

Fatigue testing:

- ROELL/AMSLER resonant pulsator
- frequency 80 to 60 Hz
- room temperature, air
- optical determination of crack length
- measurement according to ASTM E647-08 standard

Ti6Al4V

EOSINT M270 machine

- 200 W laser power
- layer thickness 50 μm
- laser speed 0.8 m/s
- scanning strategy BEAM-IT
- **stress relieving 380 °C/8 hours, argon**

Influence of heat treatment on fatigue crack growth

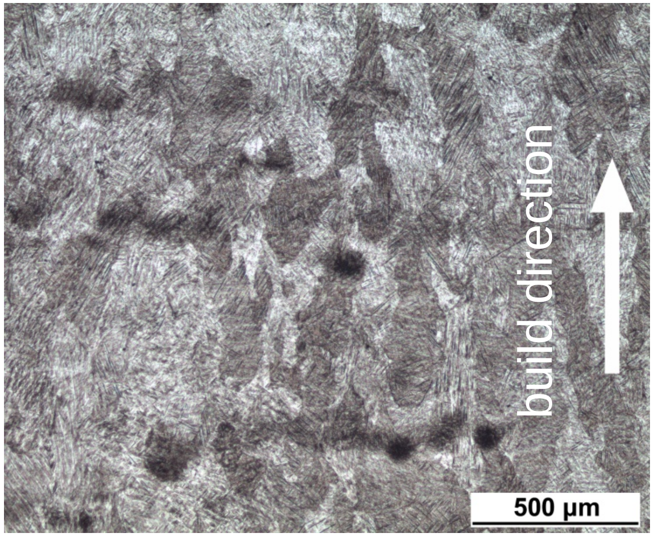

primary columnar β grains elongated in build direction

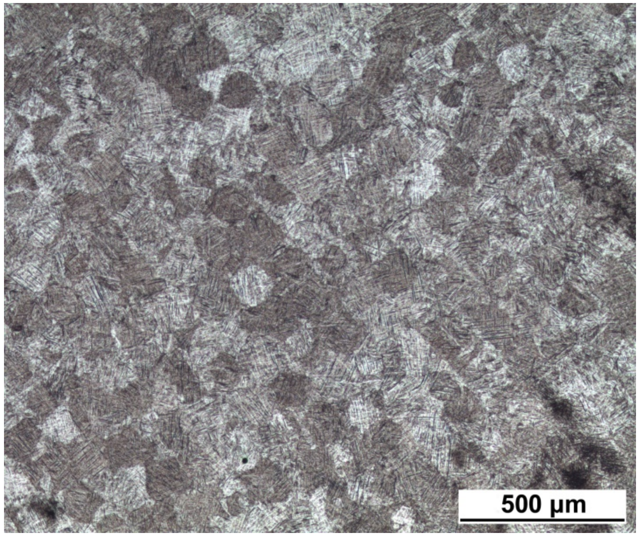

columnar structure in section perpendicular to build direction

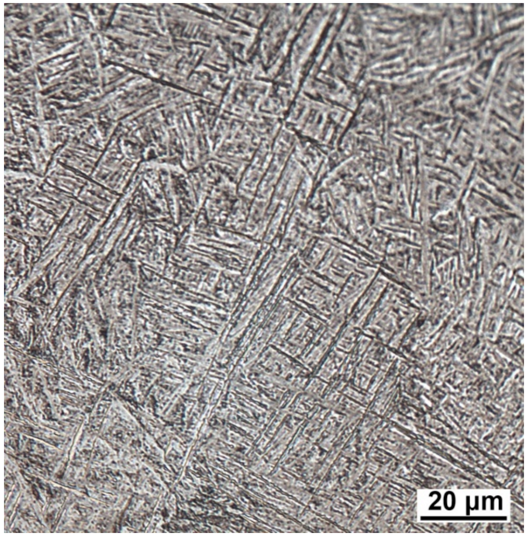

fine acicular α' martensite

Microstructure similar to that of as-built material

Ti6Al4V

Long crack growth curve

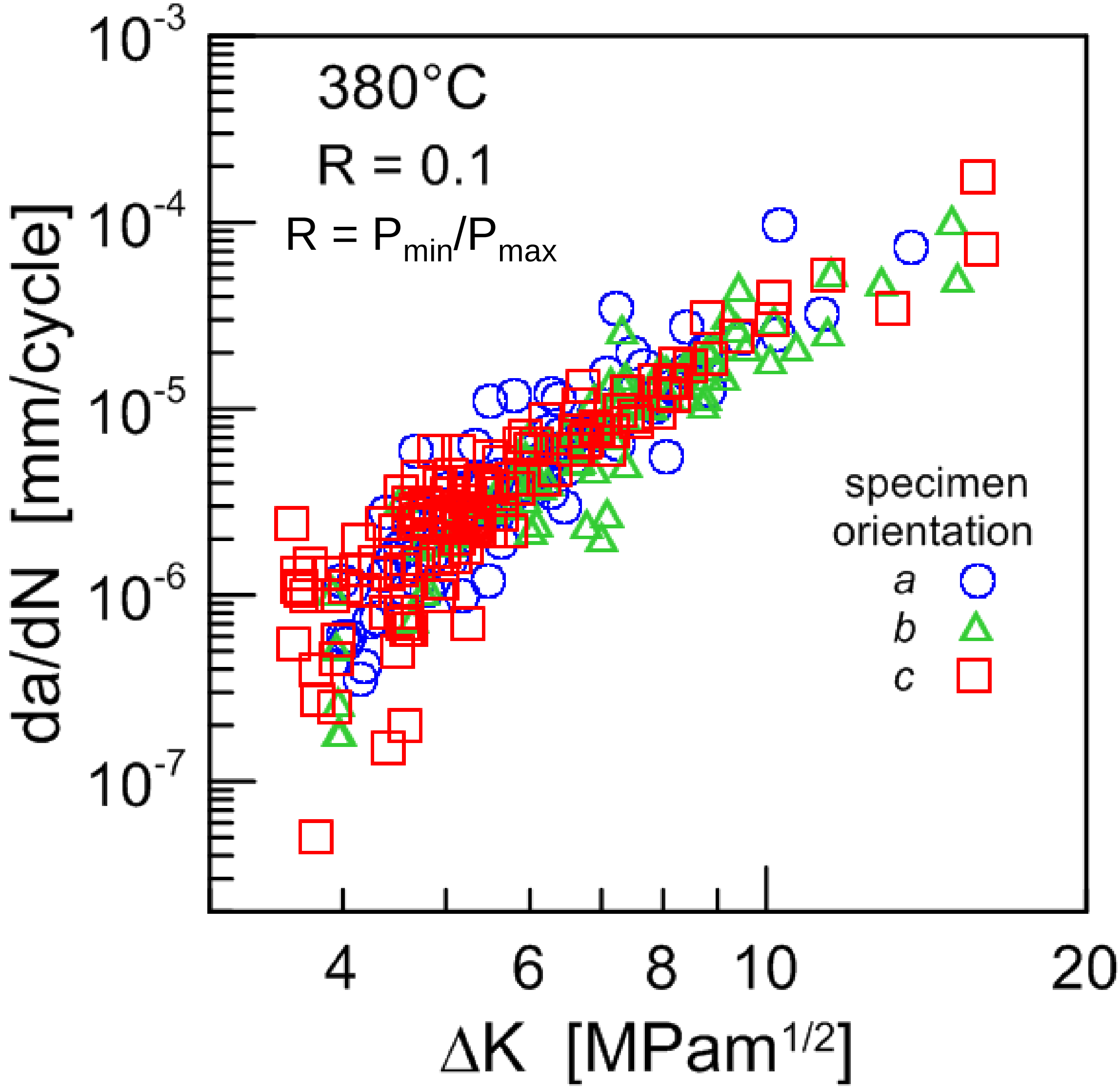

- **No influence of the building direction**
- **High scatter of experimental data**

ΔK is the stress intensity factor range characterizing the loading of the crack

Ti6Al4V

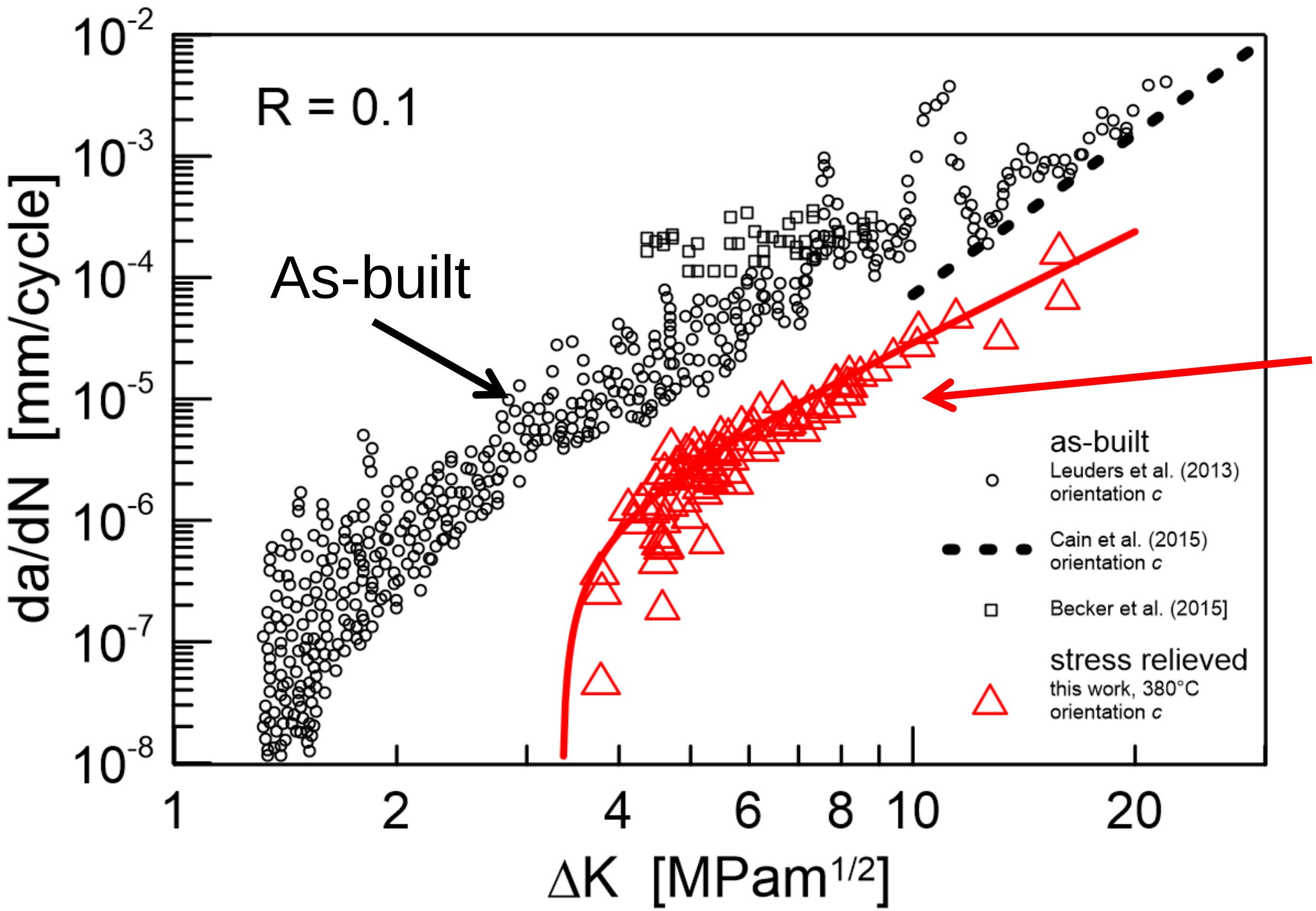

Extremely large scatter: residual stresses

Stress relieving at 380 °C:

- **higher crack growth resistance**

da/dN curves of as-built and stress relieved material, orientation c)

Residual stresses

Stress relieving at 380 °C

T direction		L direction	
σ [MPa]	τ [MPa]	σ [MPa]	τ [MPa]
2 ± 10	-2 ± 2	28 ± 6	6 ± 1

- X – ray sin^{2}ψ method
- measurement in longitudinal **L** and transversal **T** directions
- determination on polished surface and electrolytically removed 0.1 mm layer

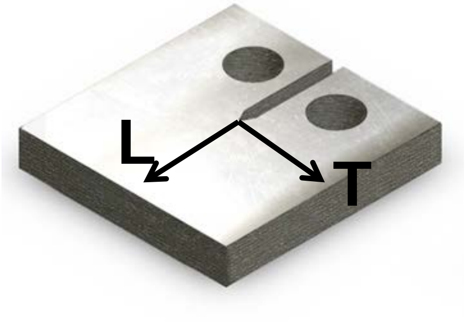

- **Heat treatment at 380 °C removes long range residual stresses**
- **Long range residual stresses seem to be not responsible for the high data scatter → the details of crack growth mechanism should be further investigated**

Ti6Al4V

EOSINT M290 machine

- 400 W laser power
- laser beam diameter 70 μm
- layer thickness 60 μm
- **heat treatment: 900 °C for 2 h cooling to 520 °C and in Ar to RT**

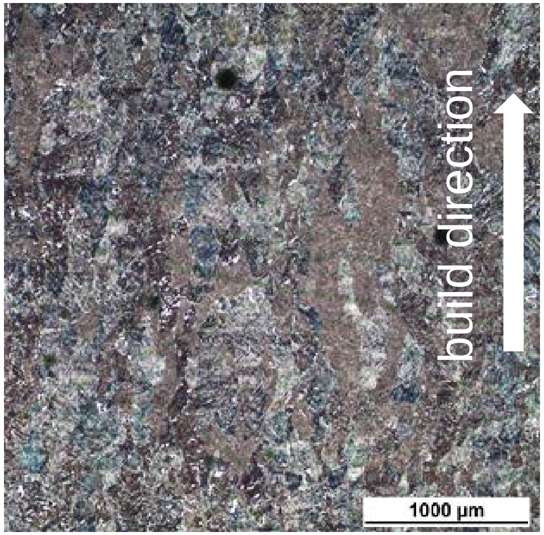

columnar structure elongated in build direction

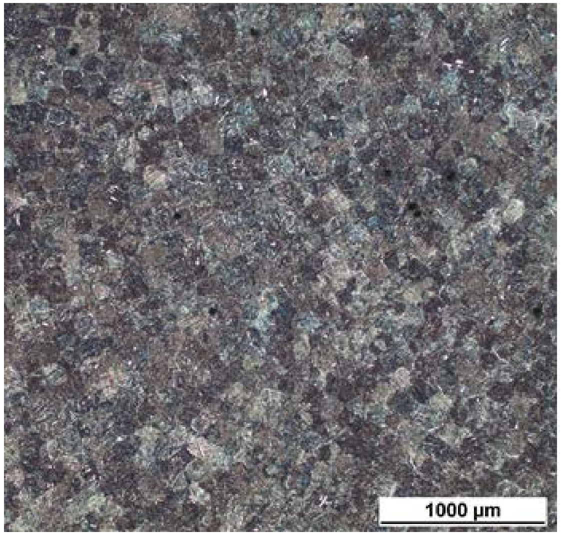

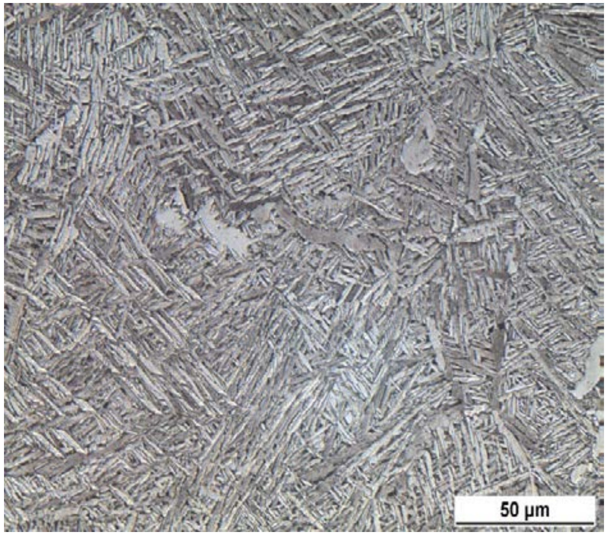

- *lamellas of α + β phases*
- *locally coarse α grains*
- *softer material*

No expressed directionality of microstructure

Ti6Al4V

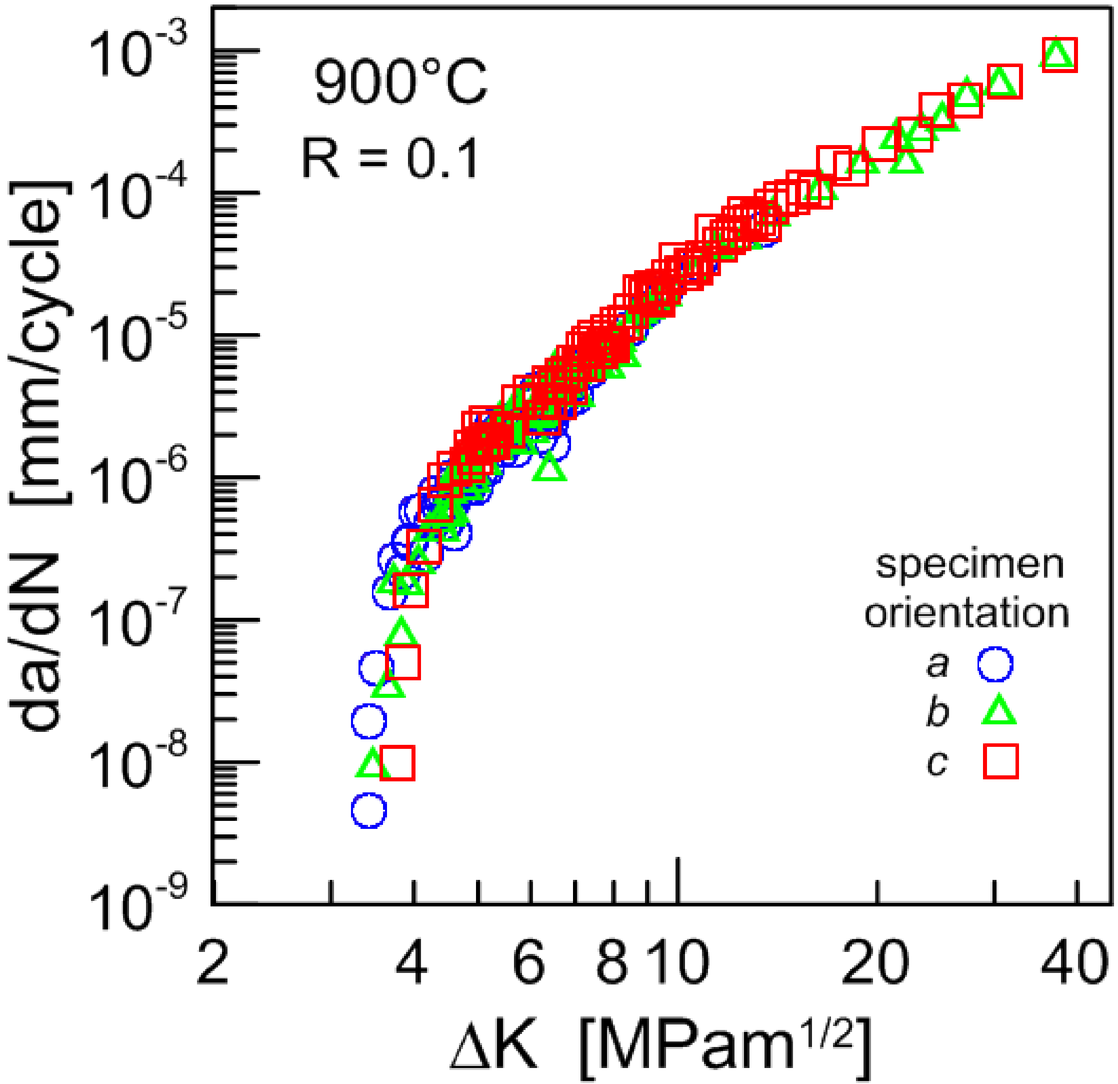

- **Crack growth is not dependent on orientation**

Ti6Al4V

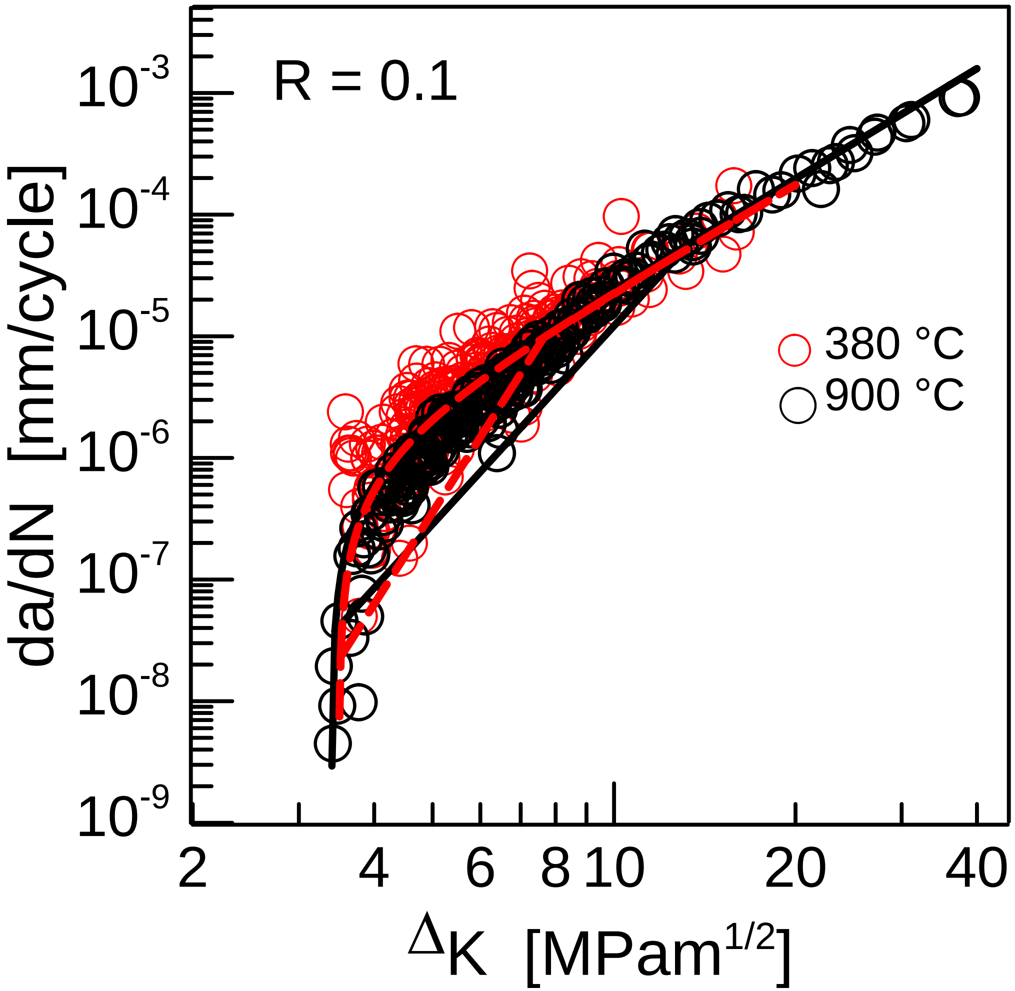

Reduced scatter of experimental points

$da/dN = 3.0x10^{-8}(\Delta K^{3.0} - \Delta K_{th}^{3.0})$ **$\Delta K_{th} = 3.5$ MPam$^{1/2}$**

$da/dN = 2.5x10^{-8}(\Delta K^{3.0} - \Delta K_{th}^{3.0})$ **$\Delta K_{th} = 3.4$ MPam$^{1/2}$**

Ti6Al4V

Heat treatment 380 °C

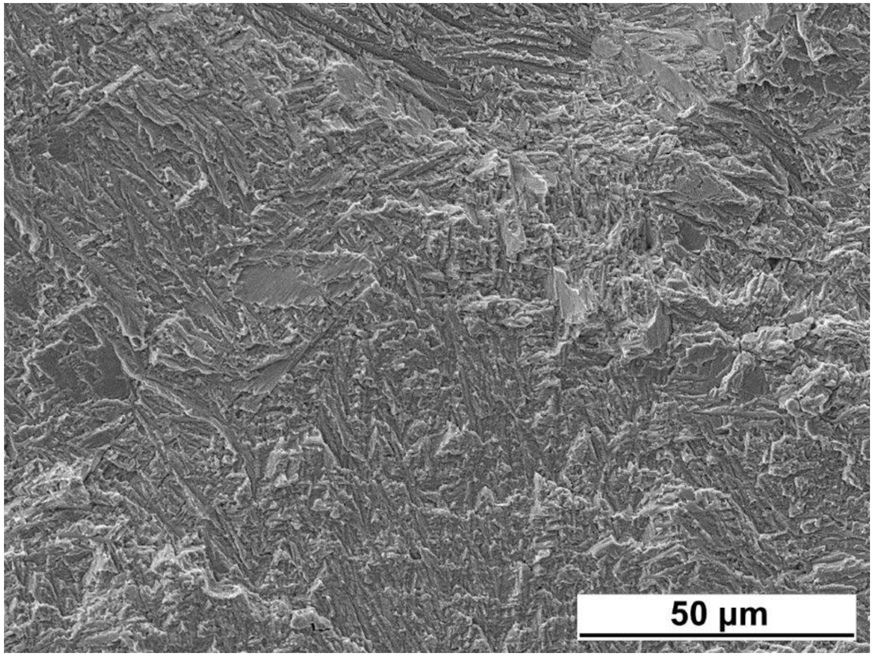

Fatigue fracture surface

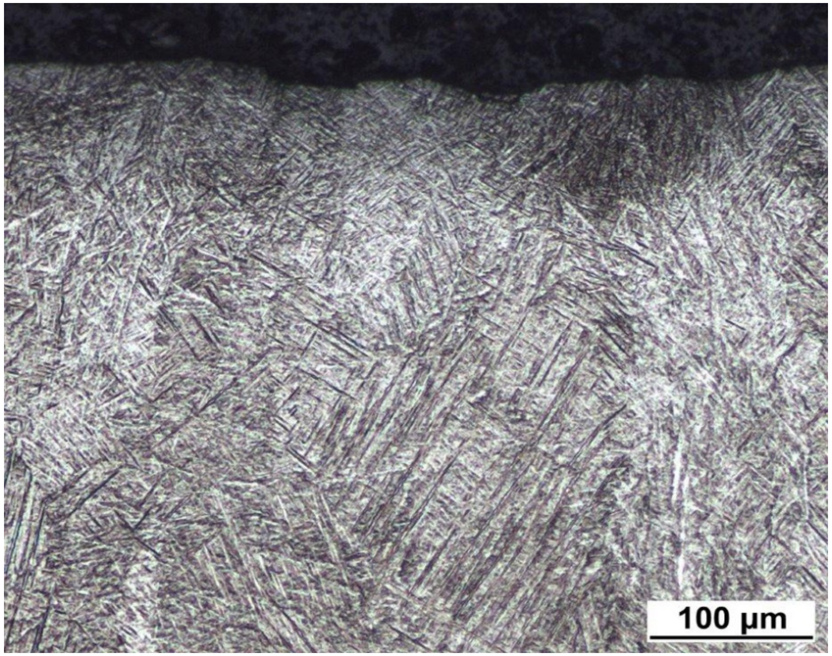

Fracture profile

Threshold region, da/dN = 10^{-8} *mm/cycle*

No apparent influence of columnar grains on the crack growth
Crack propagates by cyclic damage of fine α' martensite structure

Ti6Al4V

Heat treatment 900 °C

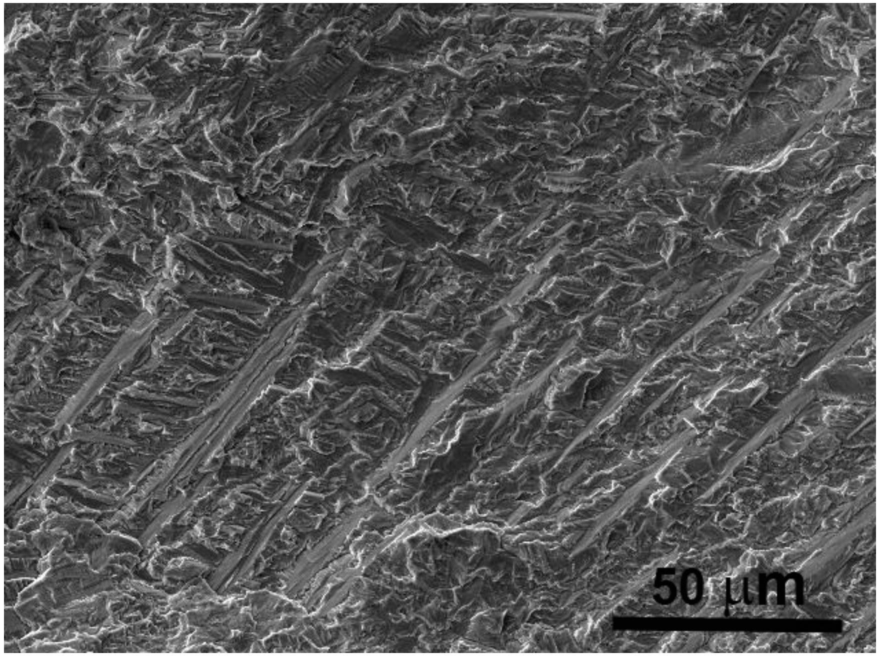

Fatigue fracture surface

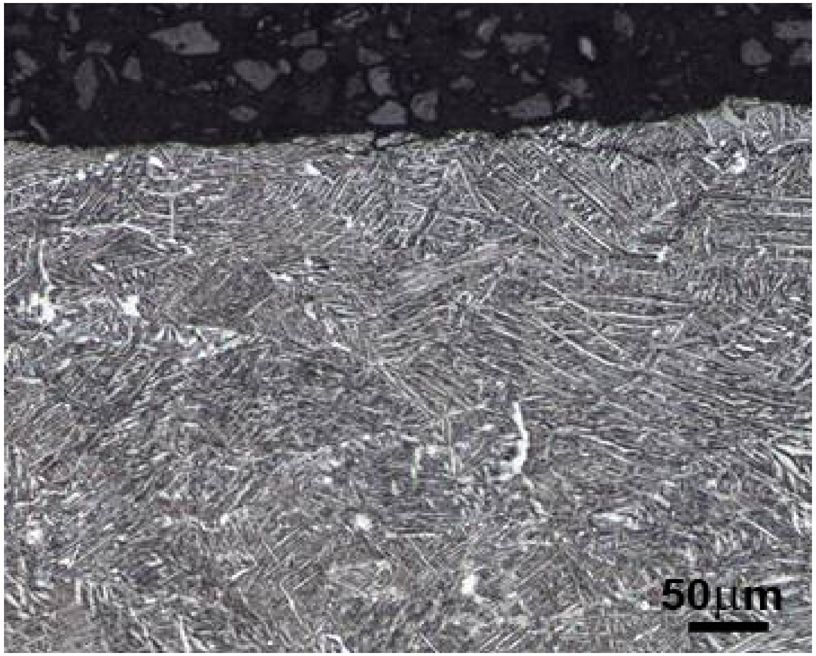

Fracture profile

Threshold region, da/dN = 10^{-8} *mm/cycle*

The crack growth mechanism consists in cyclic damage of fine α' martensite acicular structure (380 °C) or fine lamellar α + β structure (900 °C)

Ti6Al4V

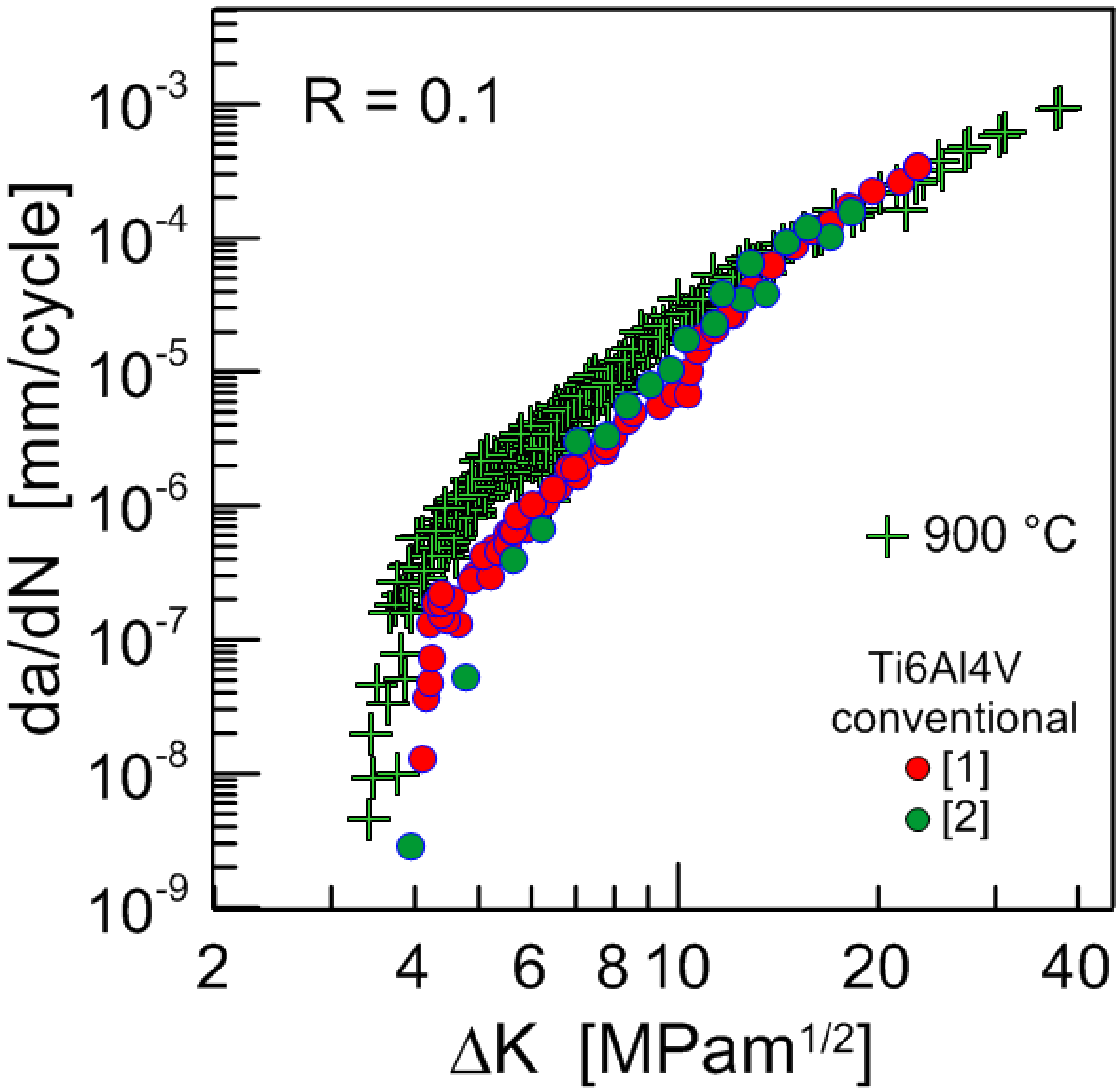

Heat treatment at 900 °C results in material comparable with that manufactured conventionally

[1] Boyce and Ritchie: Eng.Fract.Mech. 2001
[2] Oguma et al.: Int.J. of Fat. 2013

Ti6Al4V

Heat treatment 900°C

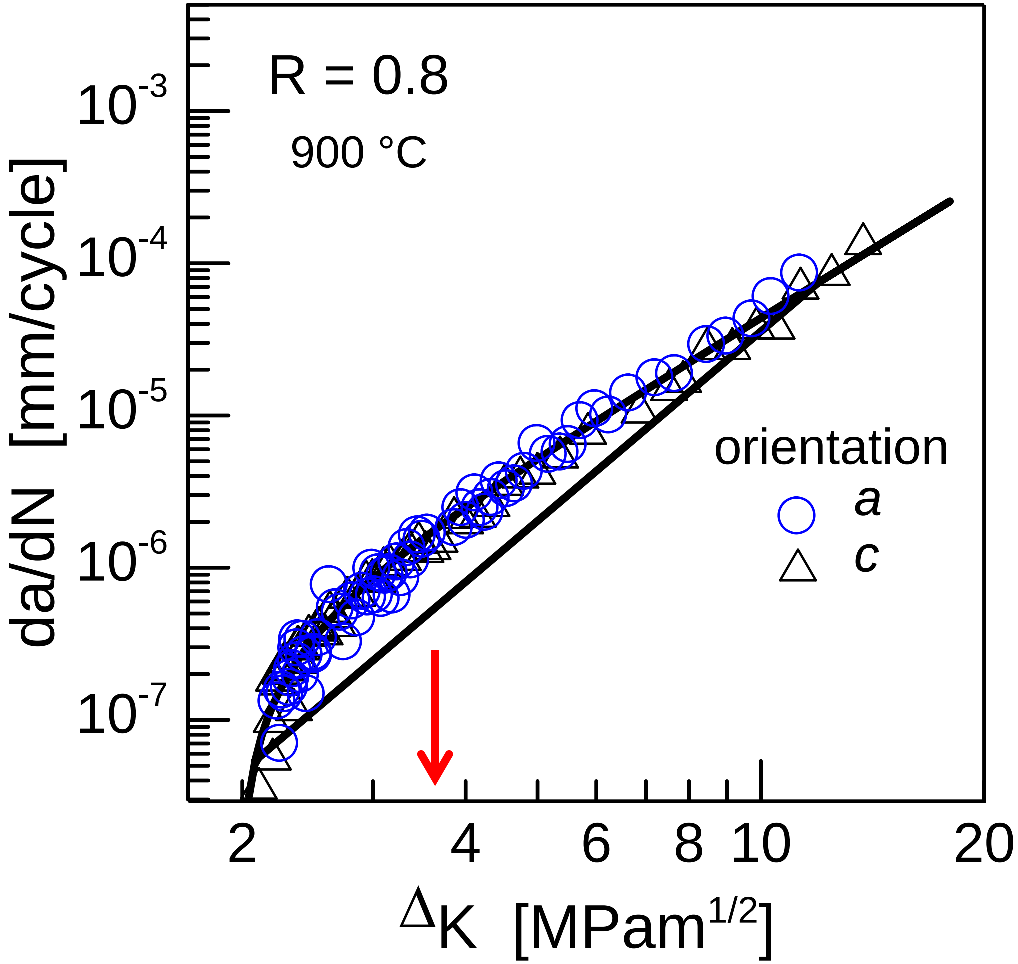

No influence of orientation

$da/dN = 4.4 \times 10^{-8}(\Delta K^{3.0} - \Delta K_{th}^{3.0})$

$\Delta K_{th} = 2.0\ MPam^{1/2}$

Ti6Al4V

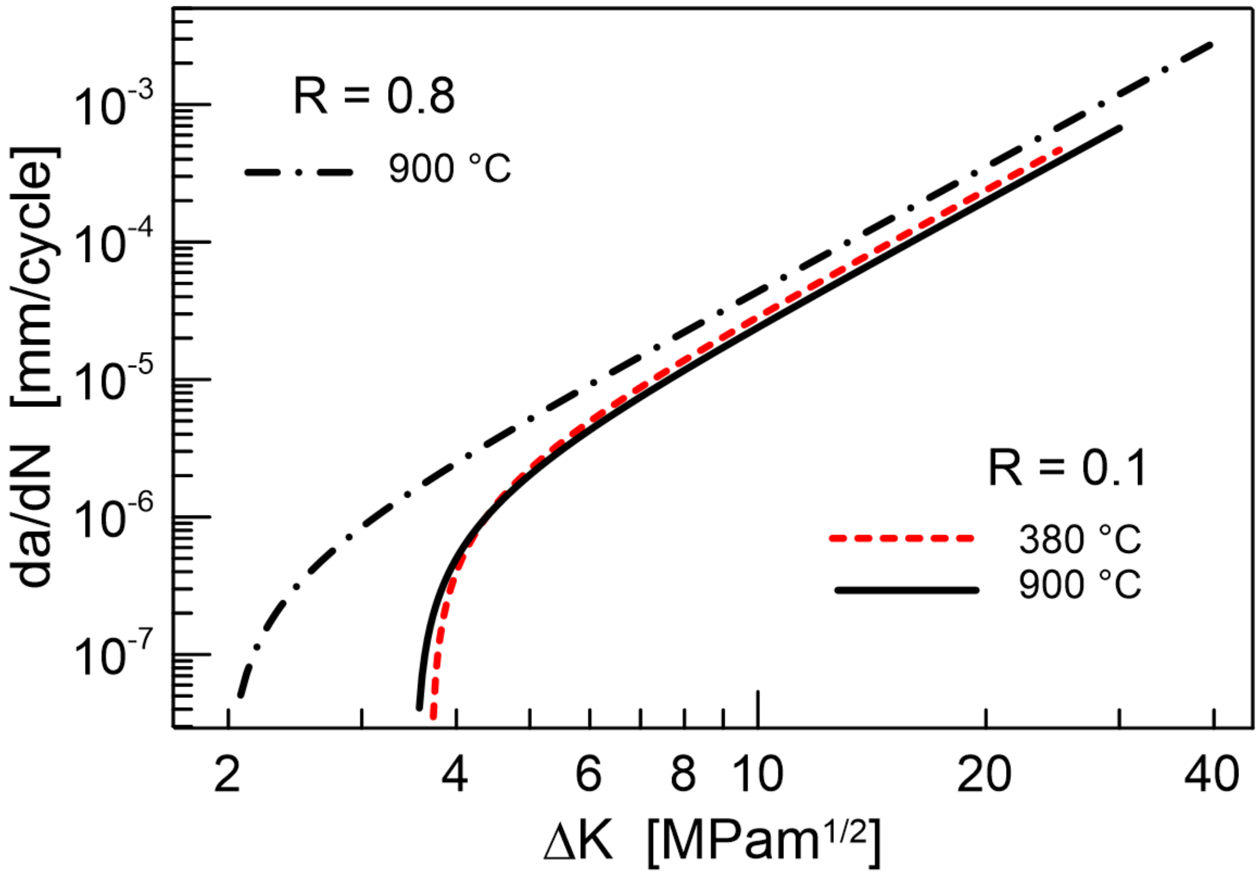

Influence of stress ratio:

- **Substantially lower threshold,**
- **Higher crack growth rate**

Ti6Al4V

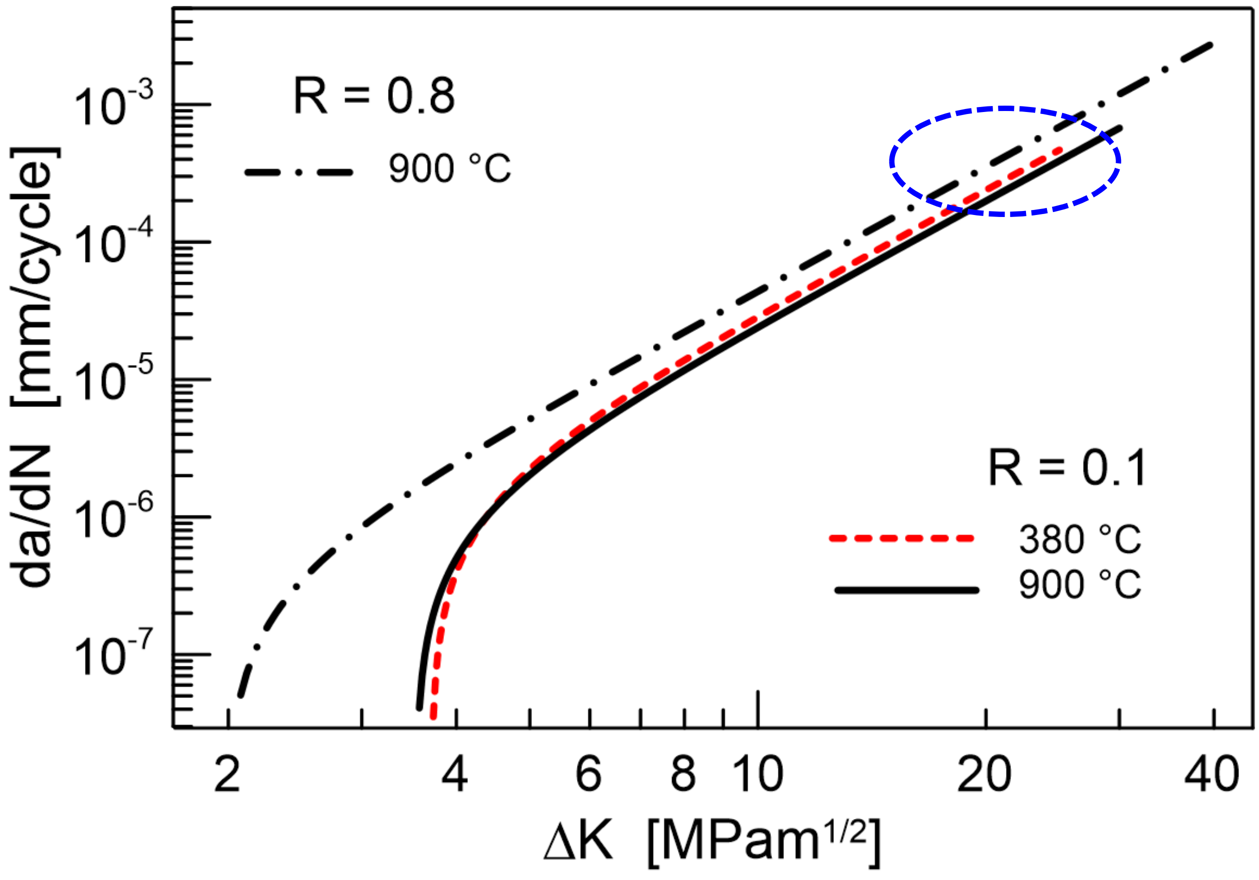

Influence of stress ratio:

- **Substantially lower threshold,**
- **Higher crack growth rate**

Ti6Al4V

Heat treatment 900°C

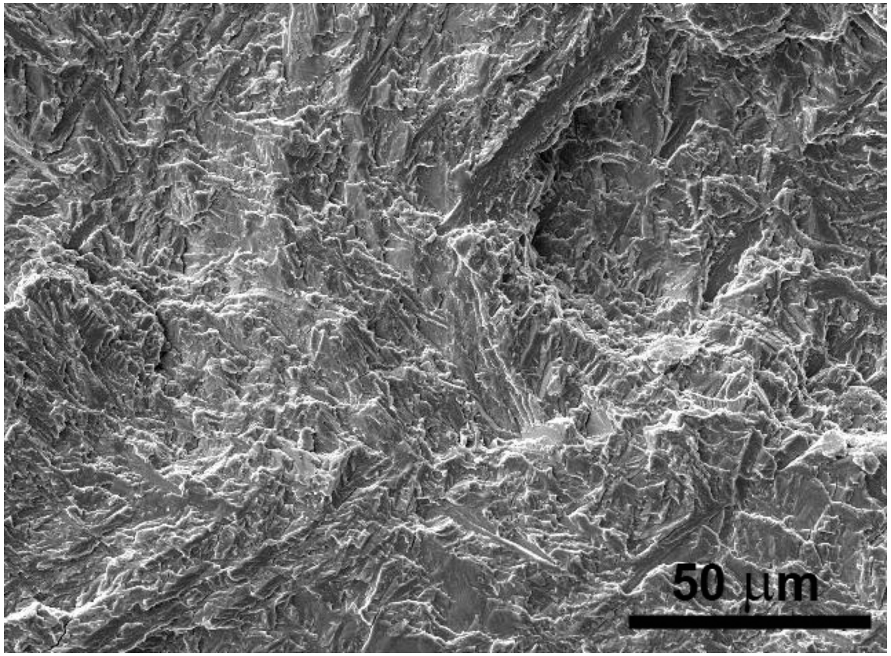

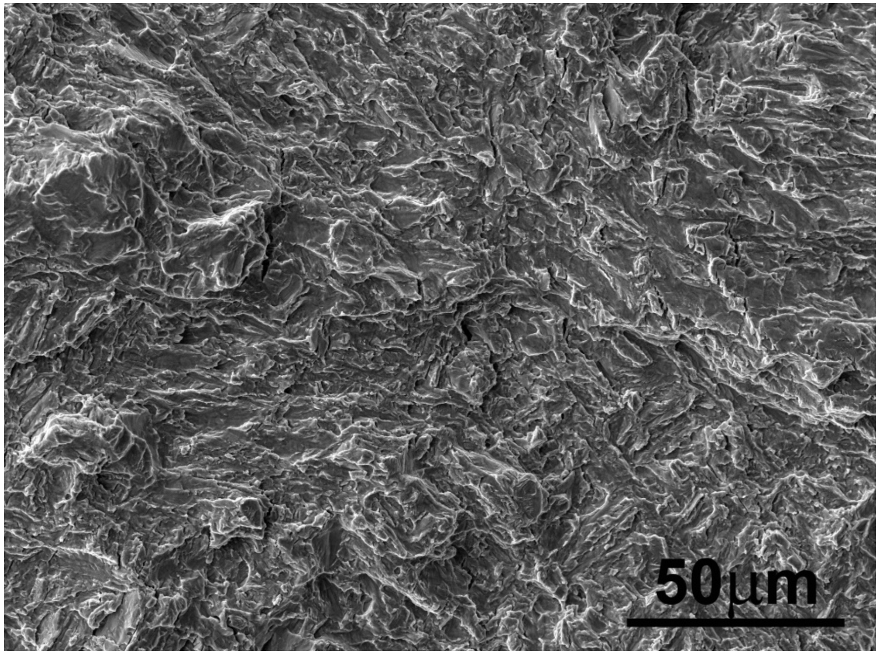

R = 0.1 *Fatigue fracture surface* *R = 0.8*

Paris region, da/dN = 10^{-5} *mm/cycle*

Similar appearance of fracture surface

Ti6Al4V

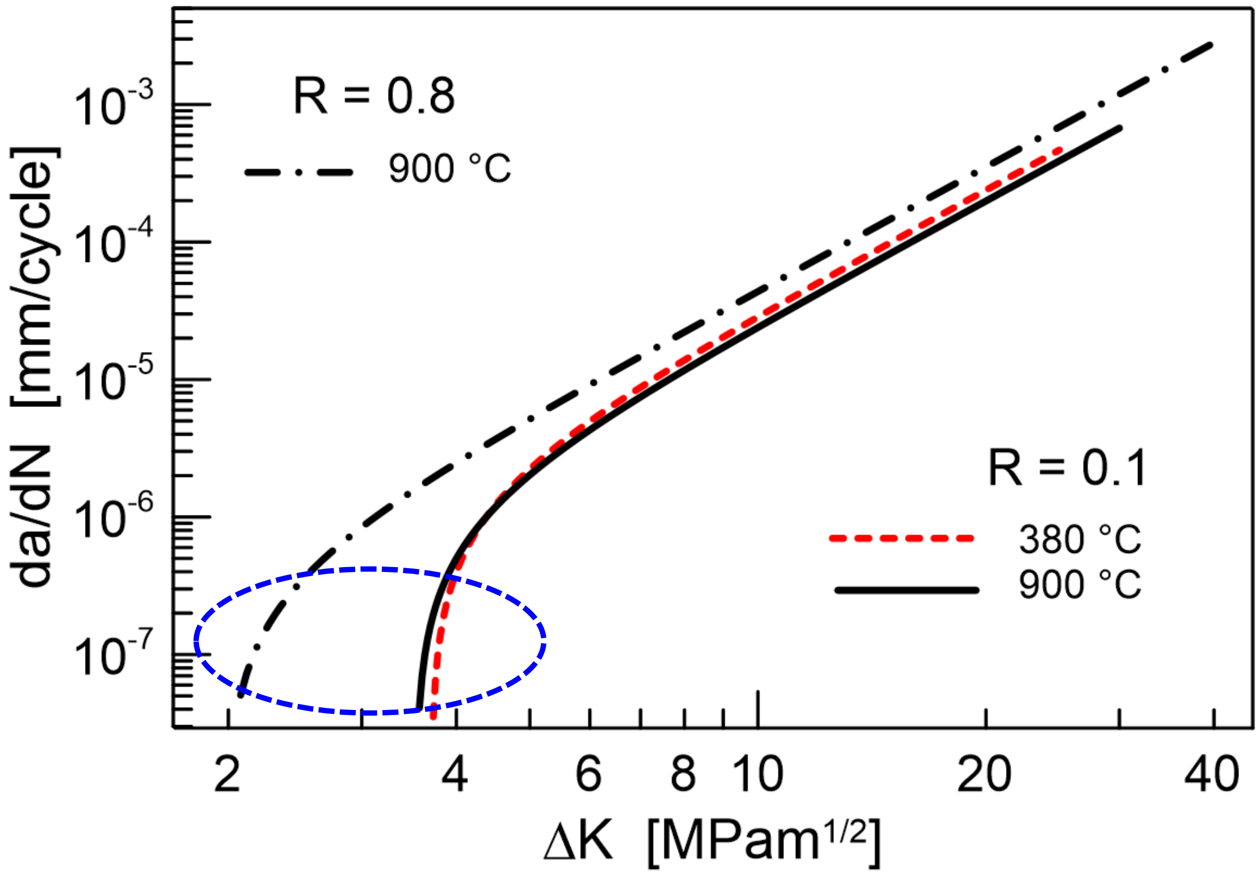

Influence of stress ratio:

- **Substantially lower threshold,**
- **Higher crack growth rate**

Ti6Al4V

Heat treatment 900°C

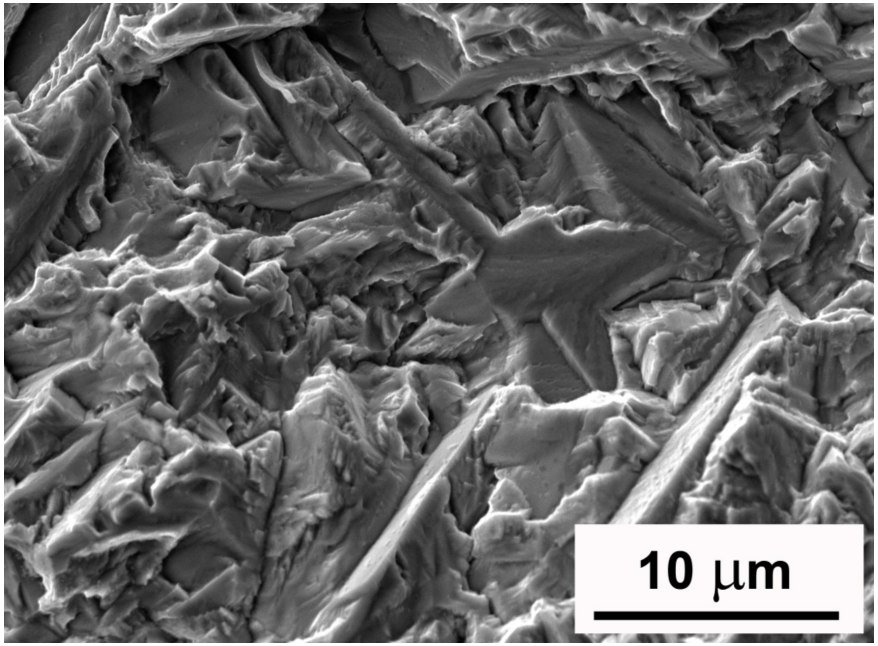

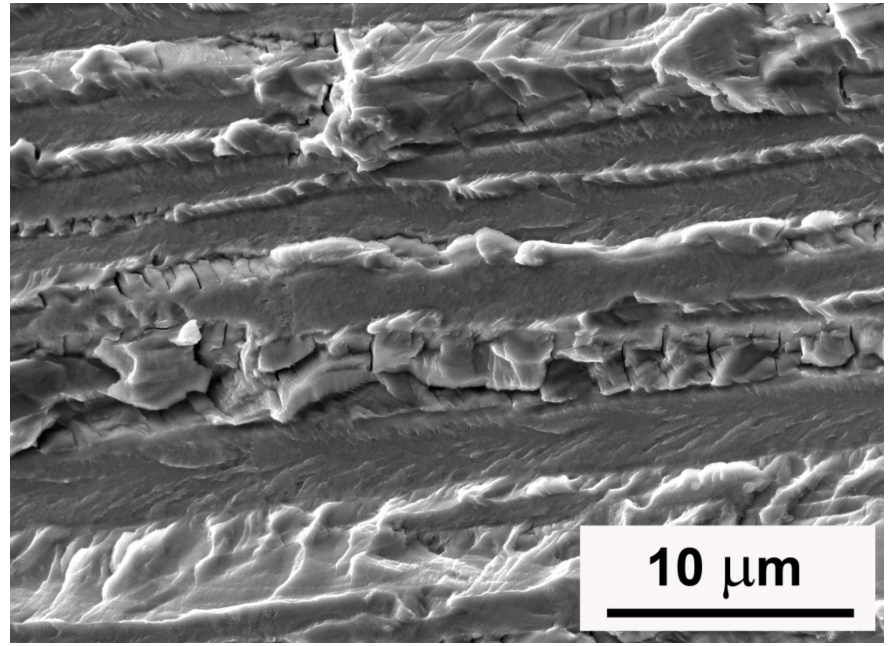

R = 0.1

Fatigue fracture surface

R = 0.8

damage along boundaries of lamellas

Threshold region, da/dN = 10^{-8} *mm/cycle*

Different crack growth mechanism

damage by „brittle“ cracking of lamellas

IN 718

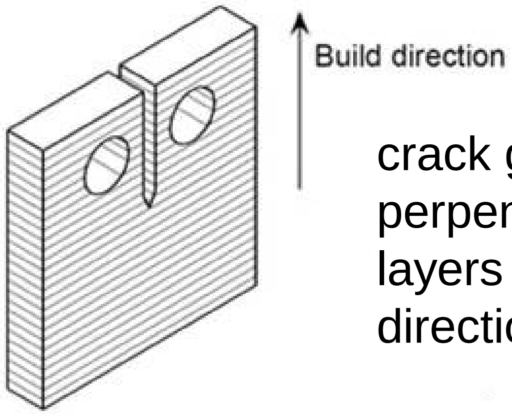

crack growth perpendicular to layers and in build direction

Specimen building:

RENISHAW 250

- 200 W laser power
- layer thickness 50 µm
- raster fashion 50 to 50 µm point-to point
- point exposure 251 µs
- scanning speed 200 mm/s
- lateral space between lines 180 µm

Fatigue testing:

- ROELL/AMSLER resonant pulsator
- frequency 80 to 60 Hz
- $R = P_{min}/P_{max} = 0.1$
- room temperature, air
- optical determination of crack length
- measurement according to ASTM E647-08 standard

IN 718

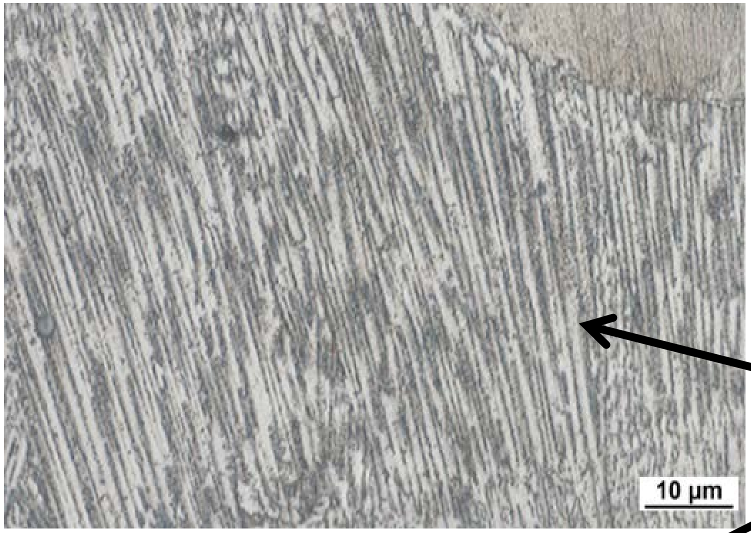

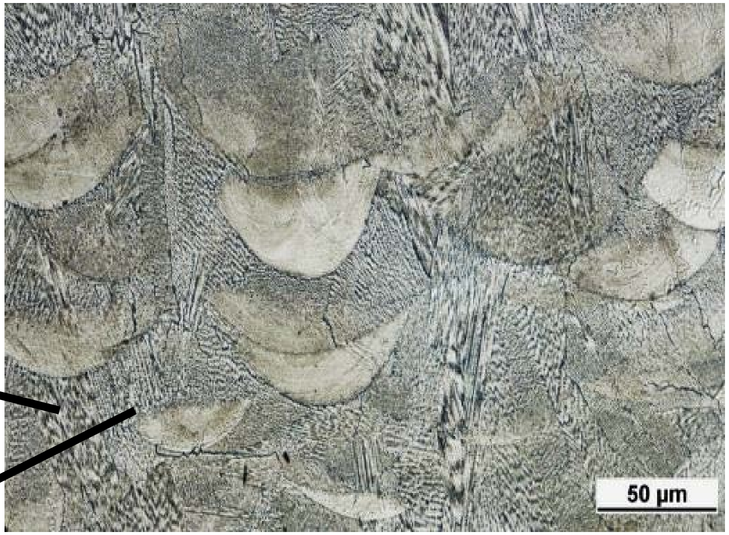

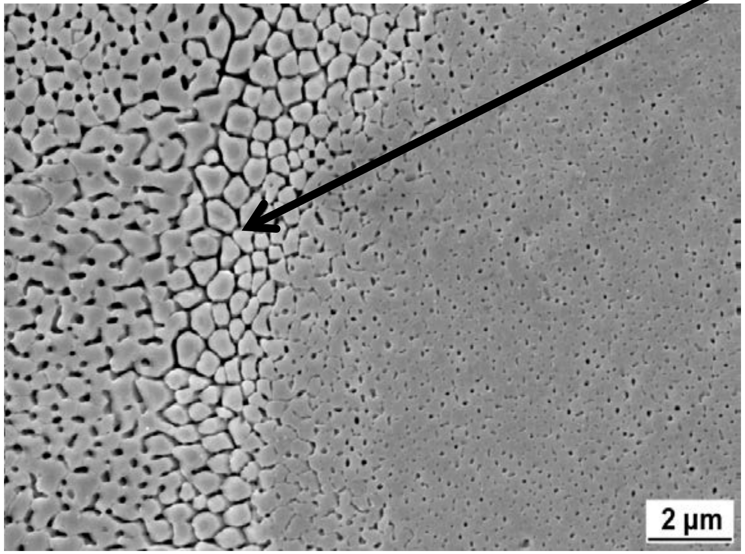

As-built state

- strong features of local solidification
- fine columnar microdendritic regions
- γ'/γ'' - cuboidal or elongated precipitates in γ matrix

IN 718

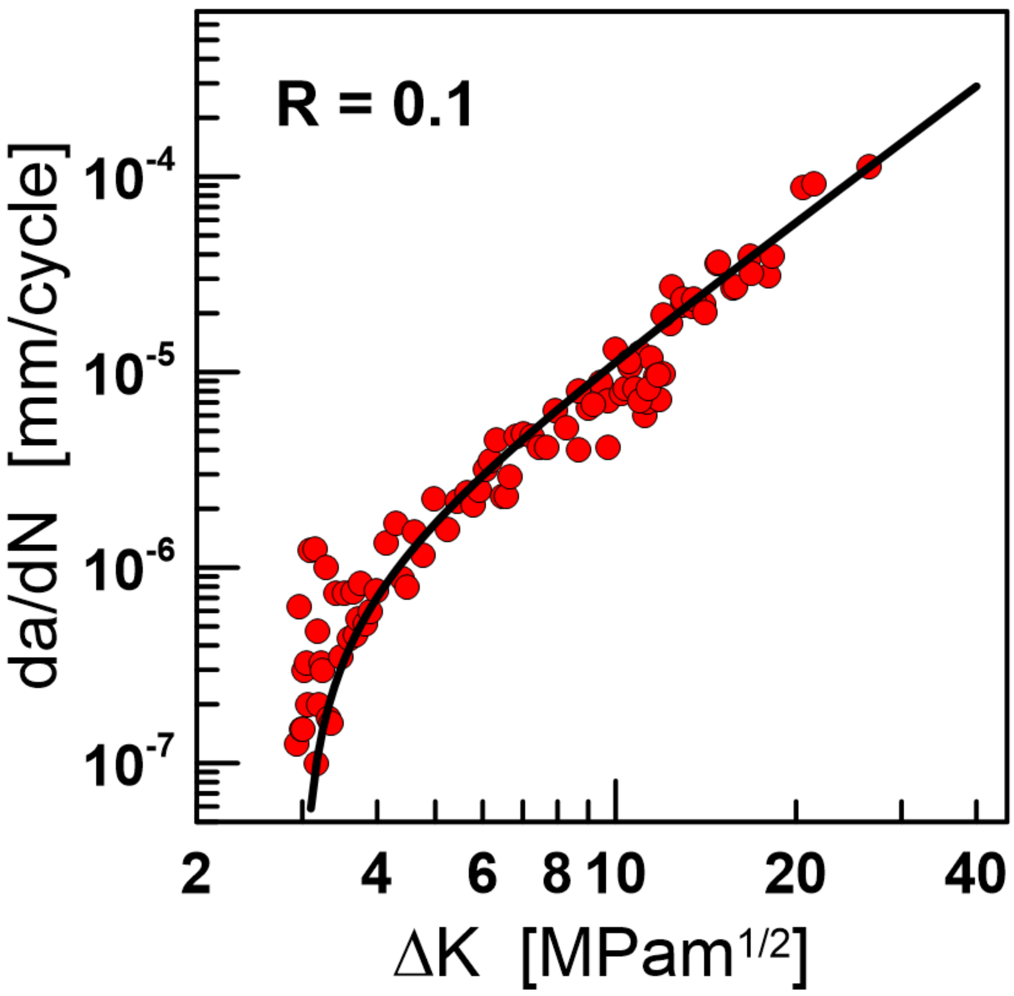

$da/dN = 6x10^{-8}(\Delta K^{2.3} - \Delta K_{th}^{2.3})$

$\Delta K_{th} = 3.0\ MPam^{1/2}$

IN 718

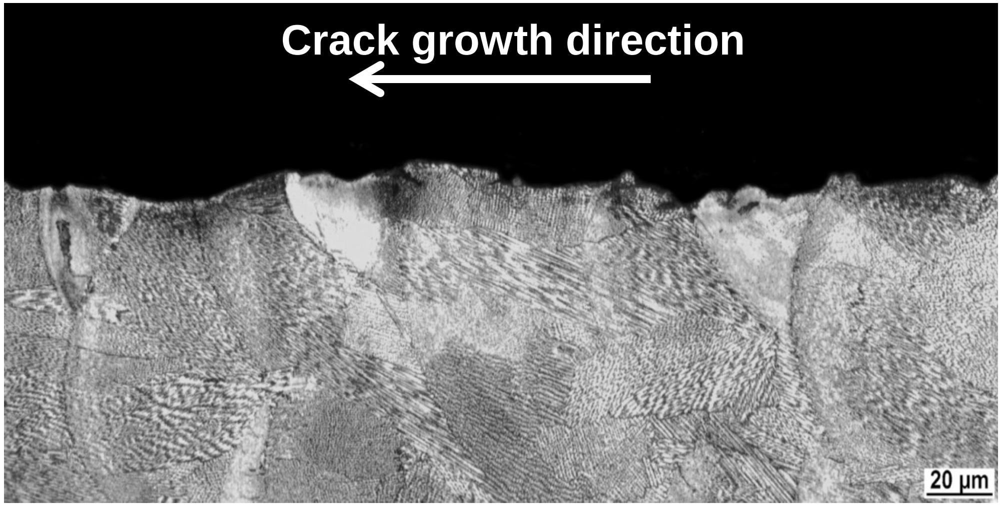

ΔK_a = 3.2 MPam$^{1/2}$, da/dN ~ 10^{-7} mm/cycle

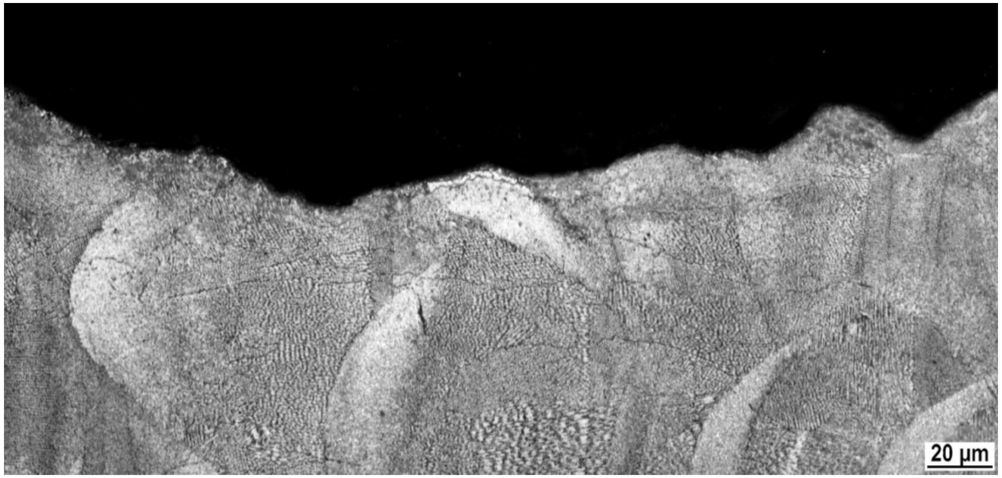

ΔK_a = 10.0 MPam$^{1/2}$, da/dN ~ 10^{-5} mm/cycle

- Transgranular crack growth
- any specific interference with grain boundaries, melt pools or building layers

IN 718

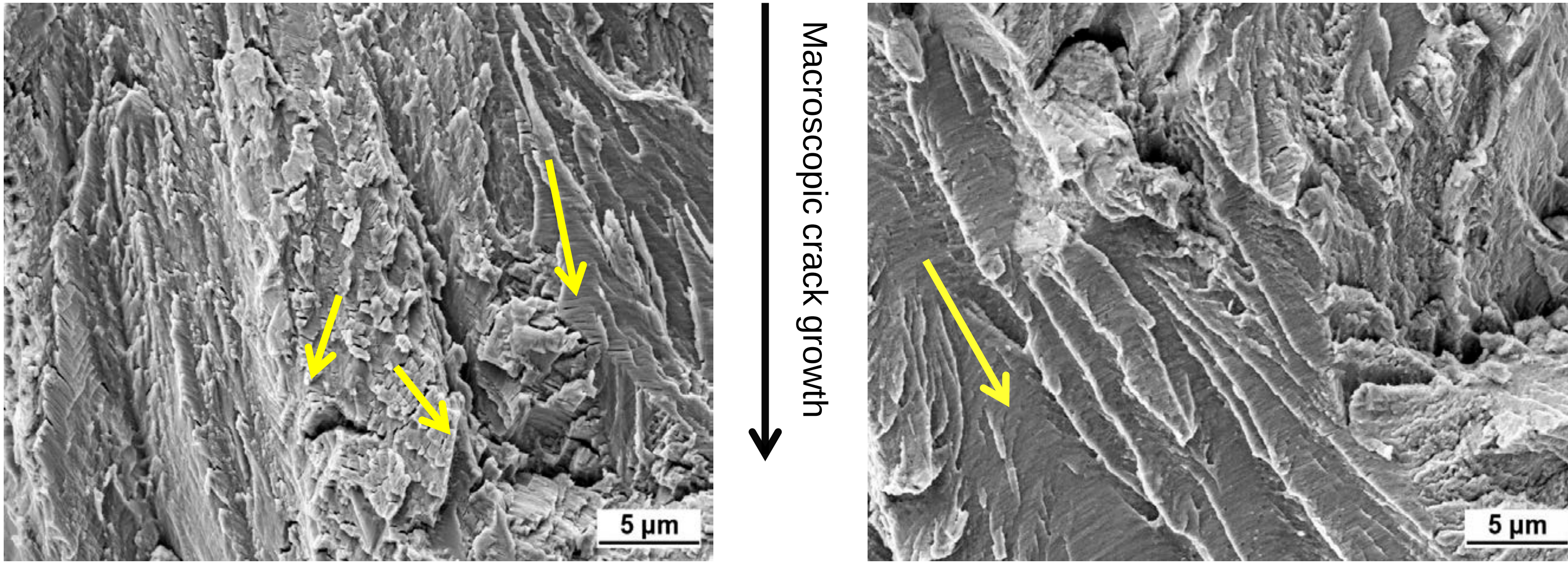

Fatigue fracture surface

Near threshold region ΔK = 4.0 MPam$^{1/2}$, da/dN = 8 x 10^{-7} mm/cycle

Mechaism of growth:

- based on planar cyclic slip,
- damage of slip bands,
- formation of microcracks
- linking of micorcracks to the main crack

IN 718

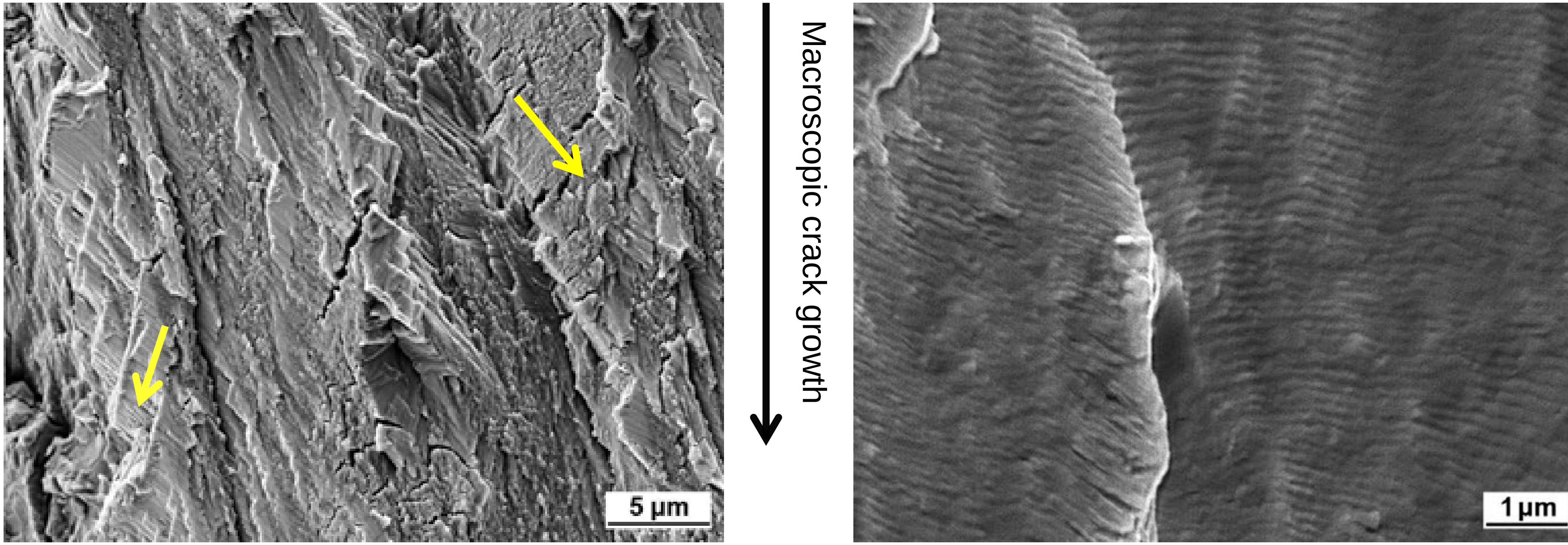

Fatigue fracture surface

Paris region $\Delta K = 10$ MPam$^{1/2}$,
da/dN = 1×10^{-5} mm/cycle

$\Delta K = 30$ MPam$^{1/2}$,
da/dN = 1×10^{-4} mm/cycle

Mechaism of growth:

- larger extent of cyclic plasticity
- more opened and larger secondary cracks
- formation of striations for highest rates

IN 718

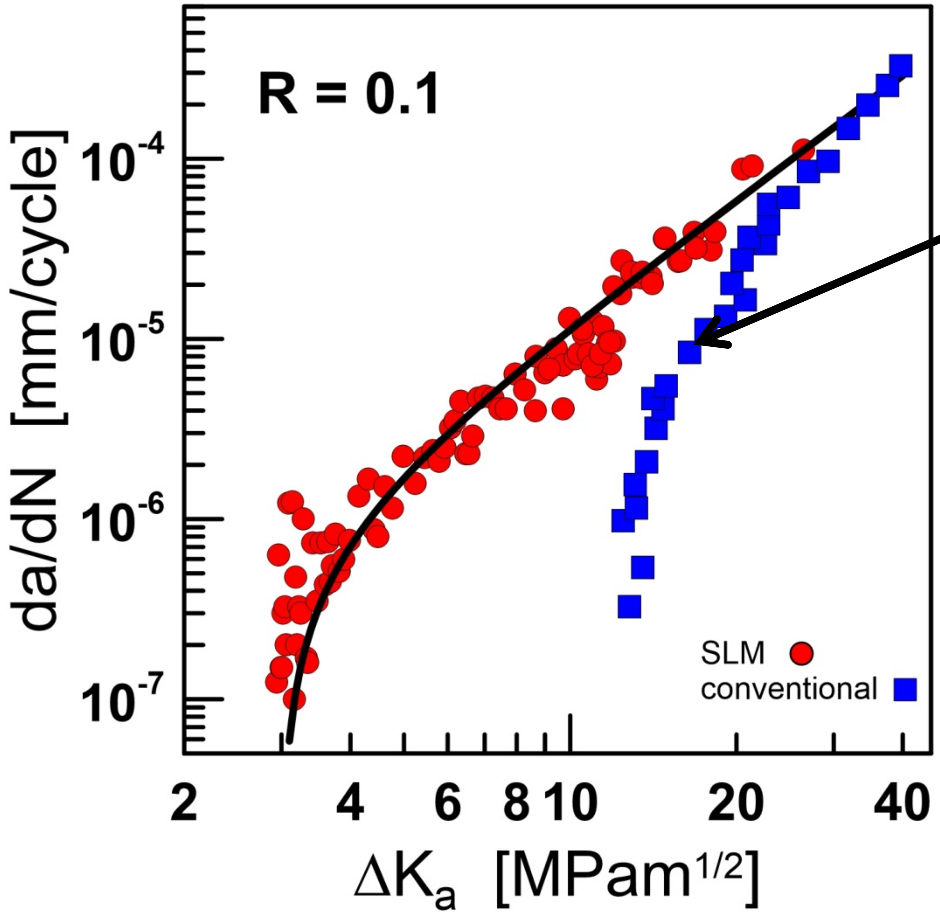

Clavel et al.
Met. Trans A
(1978) 471

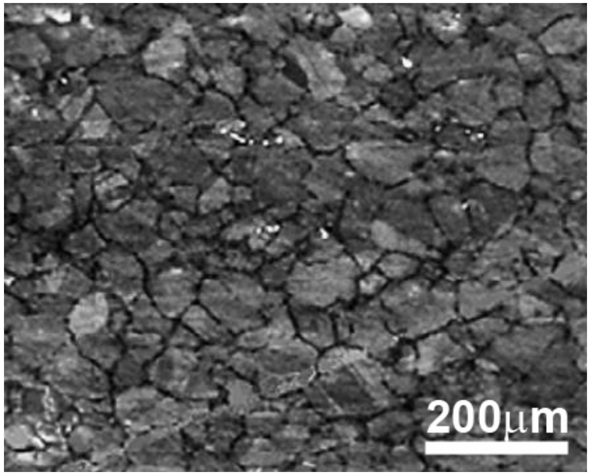

forged and heat treated material
polyhedral grains, ~30 µm

Crack growth resistance for ΔK_{th} > 20 MPam$^{1/2}$ corresponds to the conventionally manufactured alloy
Low threshold is related to the very fine structure

Influence of pre-deformation on fatigue life of Ti6Al4V

Implants are cyclically loaded, fatigue resistance and
minimum dimensions required

3D printed Ti6Al4V implants for treatment of human pelvis

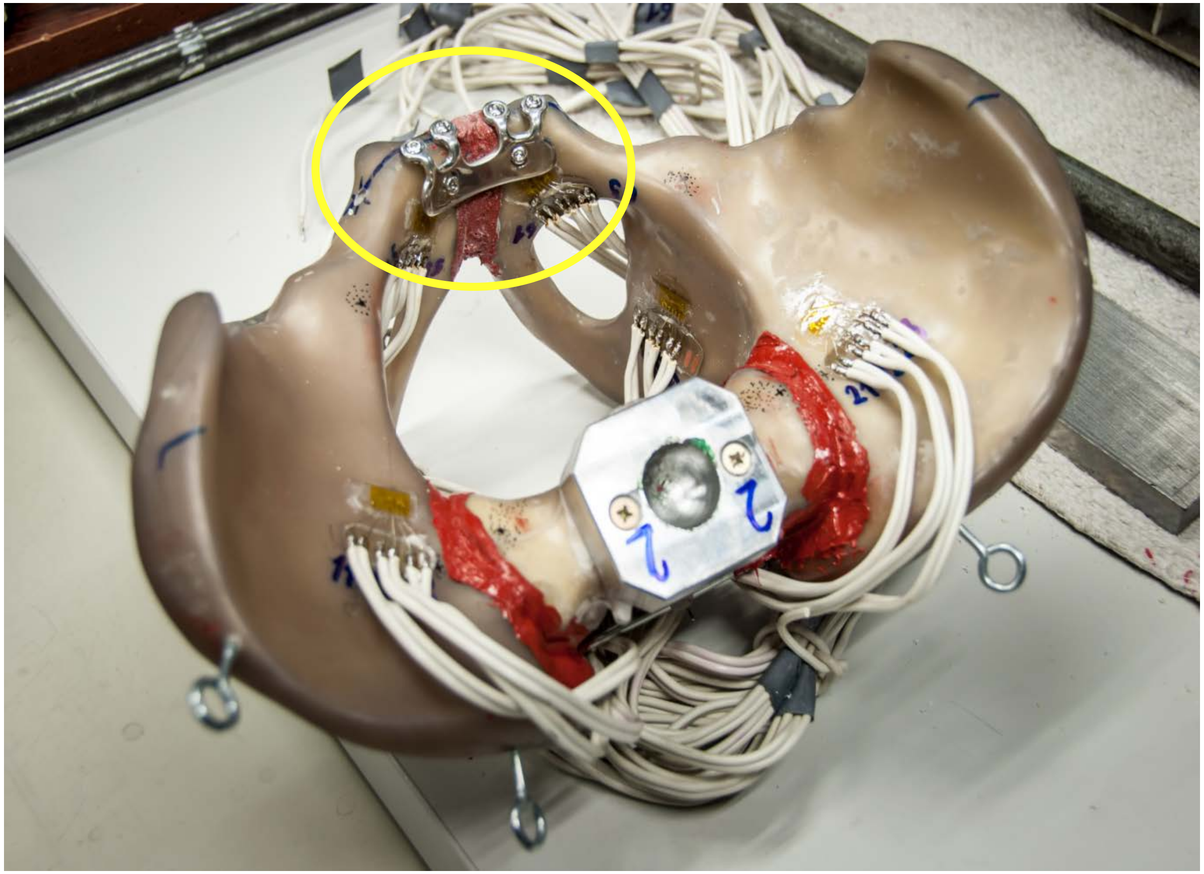

adaptation of the implant to the pelvis by bending during surgery

Pelvis model treated by 3D printed Ti6Al4V implant

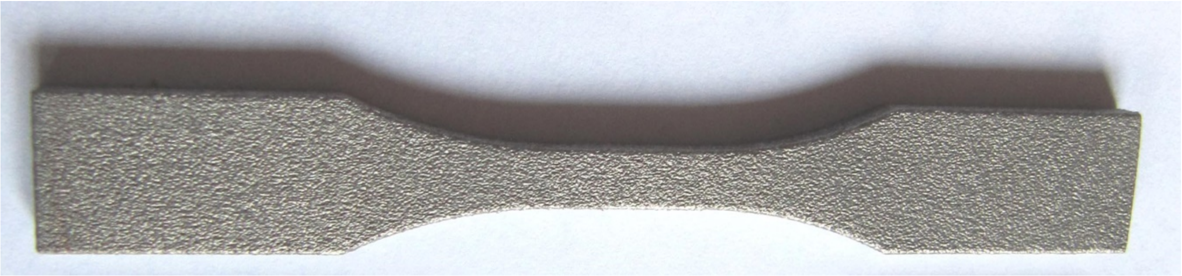

Specimens:

- specimens heat treated at 950°C for 2 h,
- corundum powder blasting and balloting

determination of fatigue life: S-N curve

- ➢ undeformed specimens
- ➢ pre-deformed 2 % plastic strain

Ti6Al4V

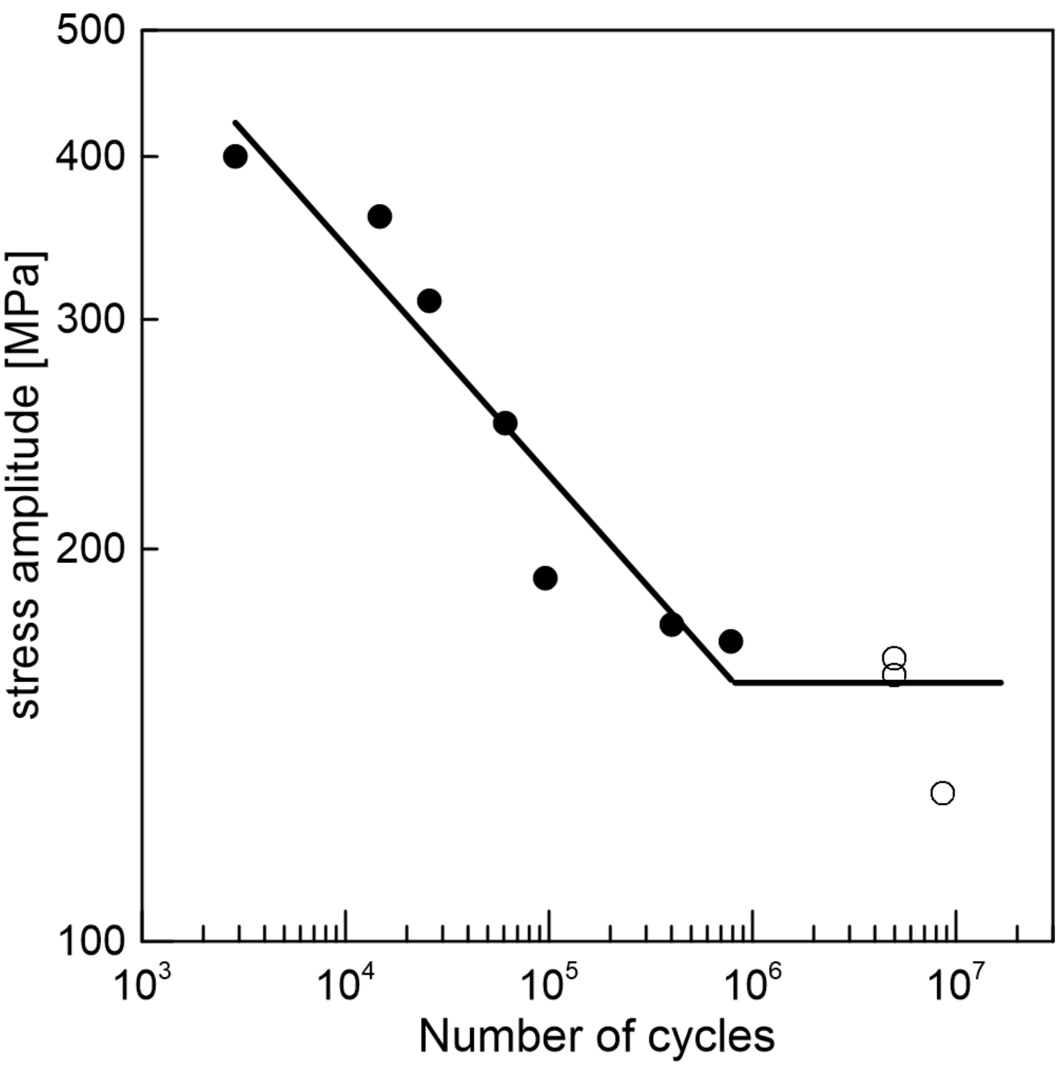

S-N curve for
R = 0

Fatigue limit
160 MPa
(based on 10^6
cycles)

Ti6Al4V

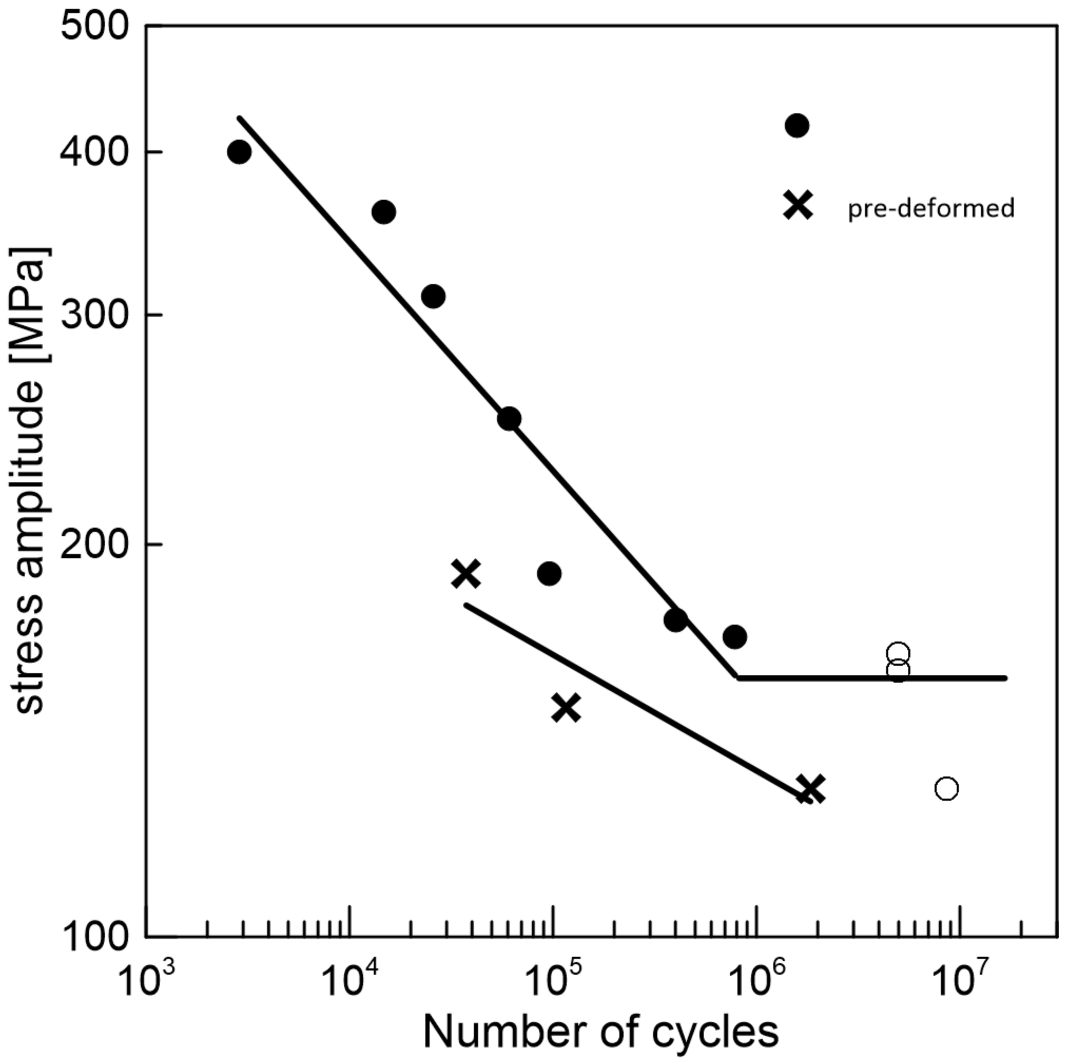

S-N curve for R = 0

Fatigue limit is substantially lower

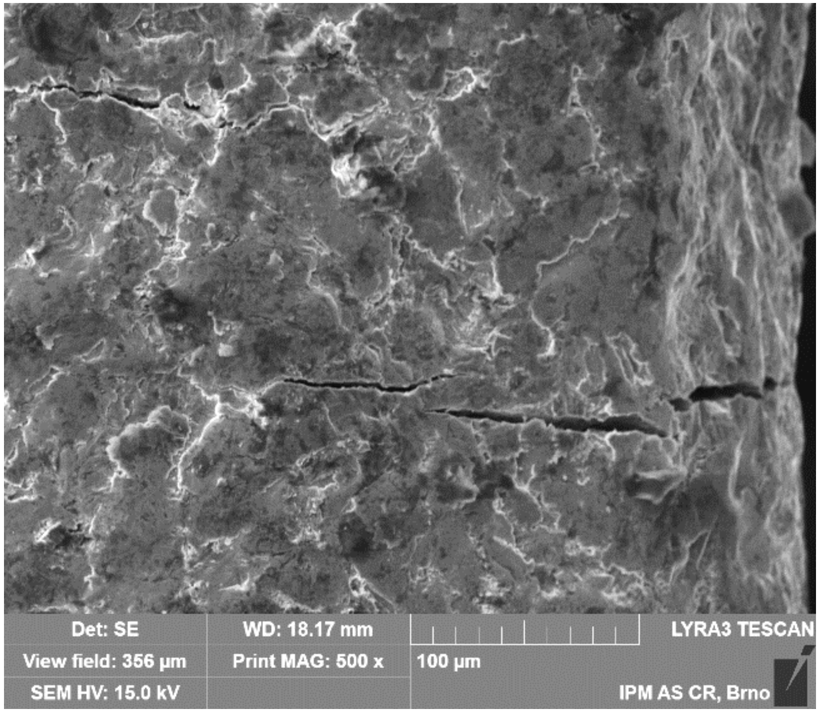

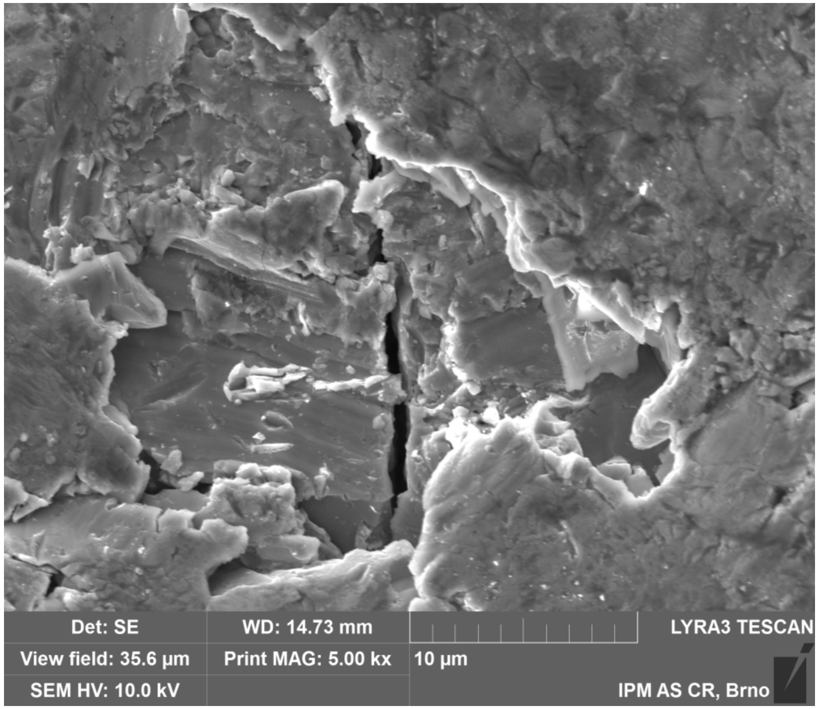

Surface cracks after plastic pre-deformation 2 %

To increase the fatigue strength, surface finishing of critical regions is necessary

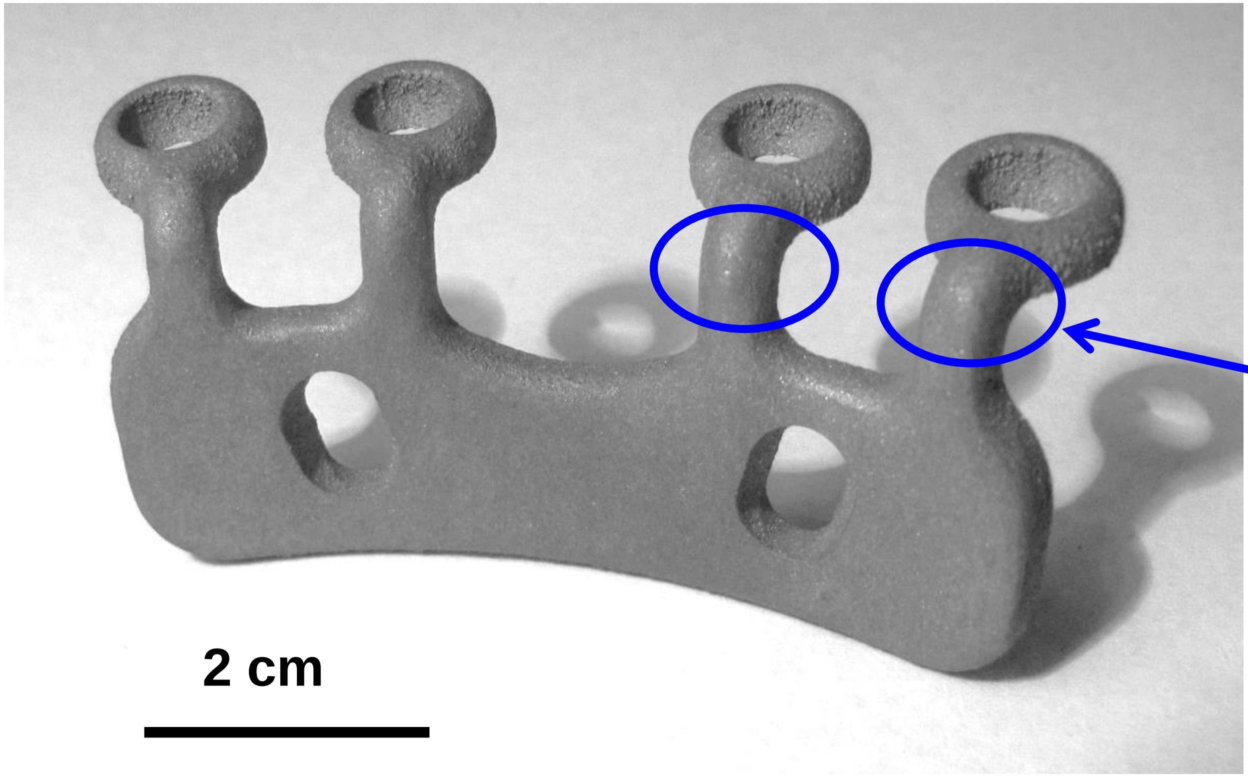

3D printed symphysis clasp

CONCLUSIONS

- **Fatigue behaviour of DMLS engineering alloys is strongly dependent on many processing parameters**

- **To get materials with good fatigue strength and good crack growth resistivity it is necessary to set optimal processing parameters and to use post-processing procedures**

- **To guarantee the fatigue properties of DMLS materials fatigue and microstructural tests has to be performed for the applied processing parameters and post-processing treatment**